NUREG/CR-3820
SAND84-1025/2 of 4
R-4
Printed August 1984

Thermal/Hydraulic Analysis Research Program Quarterly Report April – June 1984

Volume 2 of 4

S. L. Thompson, Person in Charge

Prepared by
Sandia National Laboratories
Albuquerque, New Mexico 87185 and Livermore, California 94550
for the United States Department of Energy
under Contract DE-AC04-76DP00789

Prepared for
U. S. NUCLEAR REGULATORY COMMISSION

Available from

GPO Sales Program
Division of Technical Information and Document Control
U.S. Nuclear Regulatory Commission
Washington, D.C. 20555

and

National Technical Information Service
Springfield, Virginia 22161

NUREG/CR-3820
SAND84-1025/2 of 4
R-4

THERMAL/HYDRAULIC ANALYSIS RESEARCH PROGRAM
QUARTERLY REPORT APRIL-JUNE 1984
Volume 2 of 4

S. L. Thompson, Person in Charge

Date Published: August 1984

Manager, Reactor Systems Test and Analysis Department

Director, Nuclear Fuel Cycle Programs

Sandia National Laboratories
Albuquerque, NM 87185
Operated by
Sandia Corporation
for the
U. S. Department of Energy

Prepared for
Reactor Systems Research Branch
Division of Accident Evaluation
Office of Nuclear Regulatory Research
U. S. Nuclear Regulatory Commission
Washington, DC 20555
Under Memorandum of Understanding DOE 40-550-75
NRC FIN Nos. A-1205 and A-1374

LIST OF CONTRIBUTORS

Lawrence D. Buxton

Rupert K. Byers

Dean Dobranich

Mildred G. Elrick

Lubomyra Nadia Kmetyk

Andrew C. Peterson

TABLE OF CONTENTS

LIST OF FIGURES

Page

LIST OF TABLES

SUMMARY STATUS REPORT

The TRAC-PF1/MOD1 independent assessment program at Sandia National Laboratories (SNLA) is part of a multi-faceted effort sponsored by the Nuclear Regulatory Commission (NRC) to determine the ability of various systems codes to predict the detailed thermal/hydraulic response of LWRs during accident and off-normal conditions. This program is a successor to the RELAP5/MOD1 independent assessment project underway at Sandia for the last two years.

The TRAC-PF1/MOD1 code [1] will be assessed against data from various integral and separate effects experimental test facilities, and the calculated results will also be compared with results from our previous RELAP5/MOD1 independent assessment analyses whenever possible.

The first quarter of FY84 marked the beginning of the TRAC-PF1/MOD1 independent assessment project at SNLA. The code was obtained from Los Alamos National Laboratory (LANL) in October, and brought up on both our Cyber-76 and Cray-1S computers. The assessment matrix was formalized, several TRAC nodalizations for the various facilities required have been developed, and limited calculations were begun, all described in the last quarterly [2]. During the next quarter [3], more nodalizations were developed and calculations begun, a number of user guidelines on modelling abrupt area changes and orifices were established, and the first PF1/MOD1 assessment analysis was completed [4]. We are continuing nodalization development and assessment calculations, and have now developed some guidelines for correctly using the separator model in TRAC in steady state calculations.

During this quarter, we completed a sequence of calculations investigating TRAC's ability to model horizontally stratified, cocurrent flow, for comparison with experimental data produced at Northwestern University. We found that TRAC-PF1/MOD1 correctly predicts the qualitative effects of changes in experimental conditions. Our studies also showed that liquid-to-interface heat transfer is primarily responsible for discrepancies between experimental and calculated results in the situations we analyzed. As the relative dominance of that term decreases, better agreement with measured results is obtained. A very simple modification to the interface treatment, based on boundary-layer theory, also improves both quantitative and qualitative comparisons with data. A topical report [5] on this portion of the assessment project is being prepared.

The results of the completed NEPTUNUS pressurizer component effects test analyses [6] show that somewhat higher pressures and fluid temperatures were calculated during insurges with spray flow than were measured in the test. Contributing factors to the calculation of high pressures and fluid temperatures appear to be that the interfacial heat transfer from superheated vapor to subcooled liquid was too low, and that condensation of superheated vapor on the vessel walls during insurges was delayed until the vessel saturation temperature increased above the wall temperature.

Sensitivity studies were performed on both the time step used, and the type of components and number of cells used to model the pressurizer test vessel. When the maximum time step was not controlled, the calculated liquid temperatures in the volumes into which the spray was flowing were lower than the initial temperature of the spray, the coldest liquid in the vessel; however, these unphysically low fluid temperatures in some volumes did not affect the system pressure response or the fluid temperatures near the vapor-to-liquid interface. Very similar results were calculated when the test vessel was modelled with a single PRIZER (with both 4 and 13 cells), 2 PRIZERs and 1 PIPE, and 3 PIPE components.

1.0 INTRODUCTION TO TRAC-PF1/MOD1 ASSESSMENT

The TRAC-PF1/MOD1 independent assessment program at Sandia National Laboratories (SNLA) is part of a multi-faceted effort sponsored by the Nuclear Regulatory Commission (NRC) to determine the ability of various systems codes to predict the detailed thermal/hydraulic response of LWRs during accident and off-normal conditions. This program is a successor to the RELAP5/MOD1 independent assessment project performed at Sandia during FY82 and FY83.

The TRAC-PF1/MOD1 code [1] will be assessed against data from various integral and separate effects experimental test facilities. The assessment matrix was formalized during this quarter, and is shown in Table 1.1. The calculated results will also be compared with results from our previous RELAP5/MOD1 independent assessment analyses whenever possible. A few of the tests in our TRAC-PF1/MOD1 matrix (i.e., the LOFT L2-5 and LOBI A1-04R large break tests, the PKL ID1 natural circulation test series and the B&W OTSG separate effects tests) were also in our RELAP5/MOD1 assessment matrix, and will allow such cross-comparison.

The first quarter of FY84 marked the beginning of the TRAC-PF1/MOD1 independent assessment project at SNLA. The code was obtained from Los Alamos National Laboratory in October 1984, and brought up on both our CDC Cyber-76 and Cray-1S computers; TRAC nodalizations for the PKL and B&W OTSG facilities were developed and calculations begun, as described in a previous quarterly [2]. These tests were chosen as the starting point because we had reasonably complete facility and test documentation from our RELAP5 assessment project, and we wanted some PF1/MOD1 experience with relatively simpler tests before beginning full integral system analyses such as for LOFT and Semiscale.

During the next quarter [3], a number of code problems were found in the course of the various assessment calculations; the B&W OTSG analyses were completed [4] and the PKL natural circulation analyses continued; work began on both the new (to code assessment) Bankoff/Northwestern University condensing horizontal stratified flow and the Delft University of Technology NEPTUNUS pressurizer separate effects tests; a nodalization and steady state calculation were completed for LOBI large break test A1-04R, and a nodalization was developed for Semiscale intermediate break test S-IB-3. User guidelines were developed for modelling abrupt area changes and orifices, tested for single-phase flow conditions in our PKL ID1-4 analyses and for two-phase flow conditions in our B&W OTSG study.

During this quarter, more code errors were identified and corrected, both by Sandia staff and by the code developers at LANL, as described in Section 2. Work continued on the PKL natural circulation tests, summarized in Section 3. Analyses of the condensing horizontal stratified flow tests and a NEPTUNUS pressurizer test were completed, with results given briefly in Sections 4 and 5, respectively, and in detail in topical reports [5,6]. The nodalization and steady state calculation for LOBI intermediate break test B-R1M were completed, and both the A1-04R and B-R1M transients were run until the time accumulator injection began, qualitatively summarized in Section 6 (with no actual results shown, because these test data are proprietary). Finally, Section 7 gives the status of the steady state calculations for Semiscale test S-IB-3, and the nodalization development and steady state calculations for Semiscale feedline break test S-SF-3; these Semiscale test models were used to develop and test guidelines for correctly implementing the separator model in TRAC during steady state calculations.

Table 1.1 TRAC-PF1/MOD1 FY84 Assessment Status

Test	Completed	Underway	Not Begun
LOFT			
L2-5		X	
LP-FW-1			X
LP-SB-1			X
Semiscale Mod-2A			
S-IB-3		X	
S-SF-3		X	
S-S[illegible]-5			X
Semiscale Mod-2B			
S-PL-3			X
S-SG-?			X
PKL			
ID1-4	X		
ID1-8 to 13		X	
LOBI			
A1-04R		X	
B-R1M		X	
FLECHT SEASET			
31504			X
31701			X
B&W OTSG			
28	X		
29	X		
FLECHT SEASET			
8			X
NEPTUNUS			
Y05	X		
Dartmouth			
3-tube CCFL			X
Bankoff/Northwestern Condensation			
253	X		
259	X		
293	X		
479	X		
Bankoff/Northwestern			
CCFL			X

2.0 CODE STATUS

Updates to create TRAC-PF1/MOD1 Version 11.6 from Version 11.1 were received from LANL via the user liaison Vax node this quarter. Major modelling changes are the addition of preliminary coding for the PLENUM component, which will allow multiple junctions to be connected to a single cell, and for the new generalized heat slabs, which can be used to model heat transfer between arbitrary cells in various components. (We do not plan on using and assessing these new features until LANL considers debugging and developmental assessment for them to be complete.) Numerous minor modelling changes and error corrections to previous coding were also included in the updates. Because many of the updates involved changes to the restart dump file, the graphics dump file or to common block sizes, the plot and EXTRACT utility programs used at Sandia also required modifications to be consistent with the output generated by Version 11.6.

As a first step in implementing the new version of TRAC at Sandia, the changes which affected neither our plot program nor EXTRACT were incorporated into our version of 11.1, creating an interim version approximating Version 11.4. This version was used to test various code changes and to isolate errors.

Implementation of the full 11.6 update set at Sandia was complicated by differences in deck order and common block sizes, necessitated by differences in the overlay loaders at the two labs; the inadvisability of correction idents that span more than one deck was discussed at a June 10 meeting with the developers. Final implementation of 11.6 at SNLA also required another group of updates, which contained some missing idents being modified by the original 11.6 updates and a few additional error corrections to both previous and new coding. Some of these corrections, which were received in late June, were the result of problems identified and reported by Sandia.

New changes to the time step and dump time routines created some production run problems. Consequently, our version of TRAC-PF1/MOD1 Version 11.6 includes local modifications to force both a graphics dump and a restart dump at the end of a time domain. This version also includes modifications to force a graphics dump at steady state convergence and adaptations to SNLA's overlay structure. The SNLA implementation of TRAC-PF1/MOD1 Version 11.6 is now complete and in use.

A set of updates to TRAC-PF1/MOD1 Version 11.1 was developed early this quarter to implement a current version of the utility program EXTRACT, which creates a new input deck from a TRAC restart dump file. We consider this to be a very useful utility program, but it is not currently being supported by the TRAC developers. These EXTRACT updates, plus our re-overlaying updates for TRAC, were sent to LANL in early May. By the end of the quarter, work was completed on a new version of EXTRACT, compatible with Version 11.6; it has also been sent to LANL for distribution to other users.

3.0 PKL NATURAL CIRCULATION TESTS

The Primarkreislaufe (PKL) test facility [7], located at Erlangen, West Germany, is a 1/134-scale three-loop model of a four-loop PWR. All elevations correspond to a full-scale system, so that gravitational terms are correctly simulated. Core power is provided by 340 electrically-heated rods. The ID1 series of tests [8] was designed to study the natural circulation modes occurring during small break situations in which the primary system was slowly losing inventory. In a continuous operational mode, data for twelve different inventories was recorded, with the test notations of ID1-4 to ID1-15. These data points covered the entire range of potential system response from subcooled natural circulation to reflux cooling.

The TRAC nodalization we developed for the PKL facility was described in a previous quarterly report [2], as were some preliminary calculations for the basecase natural circulation test ID1-4 which yielded single-phase flow rates significantly higher than indicated by the data. In the last quarterly report [3] we described some guidelines we developed for modelling abrupt area changes. When these guidelines were used to modify the TRAC input for test PKL ID1-4, the steady state single-phase mass flow was predicted to be exactly the same as the measured value, 4.55 kg/s, with the fluid temperatures around the loop only a few degrees higher than measured.

As also discussed in the last quarterly report [3], work was then initiated on the analysis of tests ID1-8 through ID1-15, the two-phase natural circulation test points. The preliminary TRAC calculations for 95% primary inventory reported there were based on a modified ID1-4 input deck, which reflected higher primary and secondary pressures for the two-phase tests than for the single-phase test. Those pressure boundary conditions were not directly based on the PKL data, but were instead based on our previous RELAP5/MOD1 analysis results for the 95% inventory [9].

This quarter, work was continued on the TRAC analyses for the two-phase natural circulation data points. Note that the calculations which will be reported herein were performed with a later version of TRAC-PF1/MOD1, essentially version 11.5, rather than version 11.1 as used for the ID1-4 analyses. This switch was made because several reported coding errors were fixed in the newer version. (It is our intent to perform all the final calculations for these natural circulation tests with a single, reasonably up-to-date version of the code. Depending on the frequency of receival of code updates from Los Alamos and the details of what those code updates are designed to correct, we will have to rerun either case ID1-4 or some larger subset of the calculations.)

After further analysis of the results from our initial TRAC calculation for the 95% inventory case, we decided that we would not use the pressure control approach used in the RELAP5 analyses to change from the single-phase test conditions to the considerably different two-phase ones. We thought it would be better to try to more or less directly use the measured test pressures, both primary and secondary, as boundary conditions and see if a valid two-phase natural circulation "steady state" could be achieved with TRAC.

In our first attempt to achieve a valid two-phase steady state from which to initiate further system draining, we took the quoted primary and secondary pressure values (0.300 and 0.288 MPa, respectively) for the first two-phase data point (95% primary system inventory) from the data report and applied them as boundary conditions to the original ID1-4 model. A constant pressure BREAK component was used to specify the primary system pressure control; the BREAK acted as a pressurizer and allowed flow out of and into the initially full primary system. In that first "steady state with pressurizer in" calculation, the downcomer flow went to zero very quickly, indicating that the code could not achieve a satisfactory steady state with the boundary conditions provided.

Consequently, we dropped the applied secondary pressure from 0 288 to 0.270 MPa and reran the calculation. The results of that second calculation indicated reasonably steady conditions, with a final primary system inventory of 93.7% and a downcomer mass flow rate of about 9 kg/s. The flow between the pseudo-pressurizer and the primary system was essentially zero when the calculation was terminated. Two-phase conditions existed in the top of the upper plenum, the hot leg and the steam generator inlet; the rest of the primary contained liquid. Although the calculated downcomer mass flow rate was perhaps a bit higher than the data would suggest for that inventory, the overall primary system conditions were considered to be acceptable as a starting point for further calculations in which the primary system would be drained to lower inventories.

The BREAK component acting as a pressurizer in the calculation discussed above was then replaced with a zero-velocity FILL component in our TRAC model. This "bottled up" the primary system, making the model more representative of the way the system was configured in the actual test series (i.e. sans pressurizer). Because the flow to the pseudo-pressurizer was essentially zero when we deactivated it, this change had little or no effect on a restart of the 93.7% inventory calculation.

Next, we performed a series of calculations in which a small amount of primary liquid was drained off and the system was allowed to reestablish steady state conditions. After draining only a couple of percent of the primary inventory, the downcomer mass flow rate increased considerably, substantially more than the data indicated. Nevertheless, we decided to drain the primary system to even lower inventories in order to determine the inventory at which the flow peaked and the magnitude of the peak flow at that inventory.

The inventories for which we now have performed TRAC analyses are 93.7%, 93.0%, 92.5%, 92.0%, 91.0%, 90.0%, 87.5% and 85.0%. The downcomer flow rate was predicted by TRAC to peak for a primary system inventory of 91.0% at about 13.5 kg/s. Those results are compared to the data in Figure 3.1, which shows the downcomer mass flow versus primary system inventory. As also indicated on that figure, the TRAC results were very similar to those obtained with RELAP5/MOD1 in our earlier assessment project [9]; RELAP5 predicted the flow to peak at about 90% inventory and about 13 kg/s, whereas the data indicates the flow peaks at about 95% inventory and about 9 kg/s.

Detailed analysis of these latest TRAC results indicates that the steam generatory secondary behavior in the calculations is also unlike the data, in that the tubes remained covered in the tests whereas the top of the steam generator tended to void considerably in the TRAC calculations and the secondary inventory did not remain constant. Therefore, we intend to renodalize the steam generator secondary and provide appropriate flow control systems during the next quarter to see if the agreement with data can be improved, although we are not sure that better secondary conditions will have a large influence on the primary system flow behavior. We also will perform calculations for even lower inventories in order to see if TRAC correctly predicts the reflux phase of natural circulation.

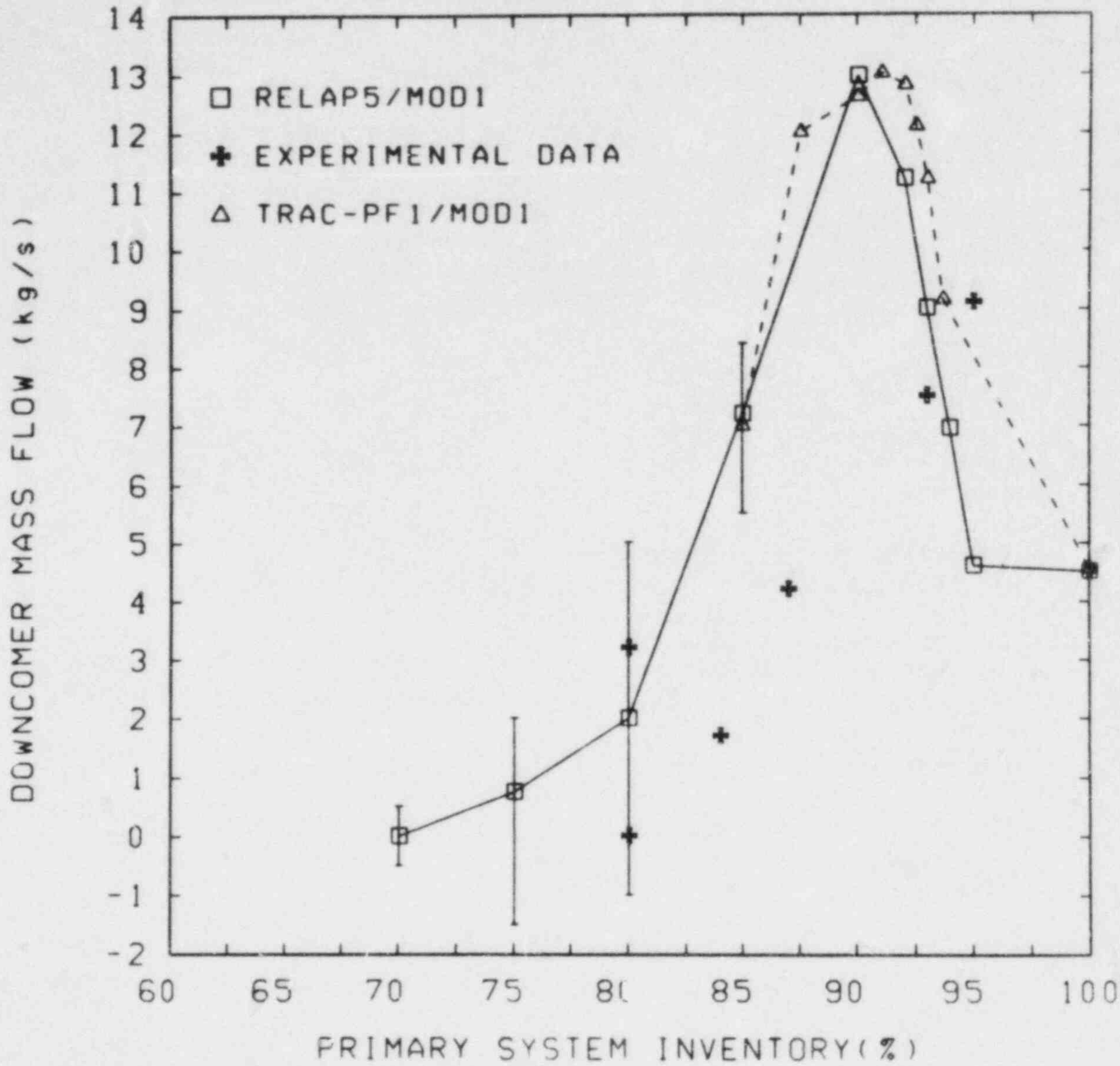

Figure 3.1 Downcomer Mass Flow vs Primary System Inventory for PKL ID1 Test Series

4.0 CONDENSATION SEPARATE EFFECTS TESTS

During this quarter, we completed a sequence of calculations investigating TRAC's ability to model horizontally stratified, cocurrent flow, for comparison with experimental data produced at Northwestern University [10]. The problem being addressed is that of flow (at roughly atmospheric pressure) in a rectangular channel about 1.6 m long, 0.3 m wide, and 0.06 m high. Heat transfer at the channel walls is assumed to be negligible. The vapor is superheated, and variations are performed on inlet flow rates, liquid level, and the amount of subcooling of the liquid (Figure 4.1). The experiments are very simple, and calculated results should display the effects of mass, momentum, and energy transfer at the interface, as well as those of wall friction.

In the last quarterly report [2], we described the results of calculations at low inlet liquid flows and low and high vapor flows, using both the standard model and simple modifications to wall shear and interfacial heat transfer for horizontally stratified flow. We have now completed a similar set at low vapor flow and high liquid flow, and at high vapor flow, low liquid flow, and high liquid inlet temperature. (These are experiments 293 and 459 in the test matrix.)

As expected, the low vapor flow, high liquid flow case showed even more "over-condensation" and countercurrent flow with the standard interfacial heat transfer coefficients (Figure 4.2); the standard liquid-to-interface term is simply proportional to the liquid velocity, and is the most dominant for this case. The lower shear coefficients in the modified calculation (Figure 4.3) result in better agreement with the experimental pressure profiles, as shown in Figure 4.4. Conversely, at high vapor flow, the liquid-to-interface heat transfer is relatively less influential, and the standard treatment gives better agreement with the data at elevated inlet liquid temperature, as shown in Figure 4.5.

We also investigated further trial modifications to the description of stratified flow, using Taylor series expansions for the velocities and taking account of both the wall and the interface. Given the ambiguity in comparing the data and calculated results (for geometric reasons), we could find no reason to expect improved results from other changes to the calculation method, and so discontinued this effort.

It appears that no purpose would be served by analyzing other experiments in the horizontal stratified flow test matrix. Our results showed that the standard TRAC treatment for this flow regime overpredicts the condensation rate when liquid-to-interface heat transfer is dominant, and that a simple modification can improve both qualitative and quantitative agreement with measured results. A topical report [5] on this portion of the TRAC assessment project is now being prepared.

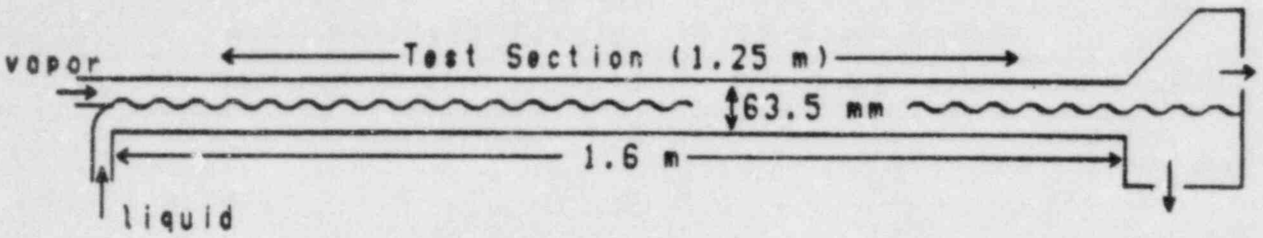

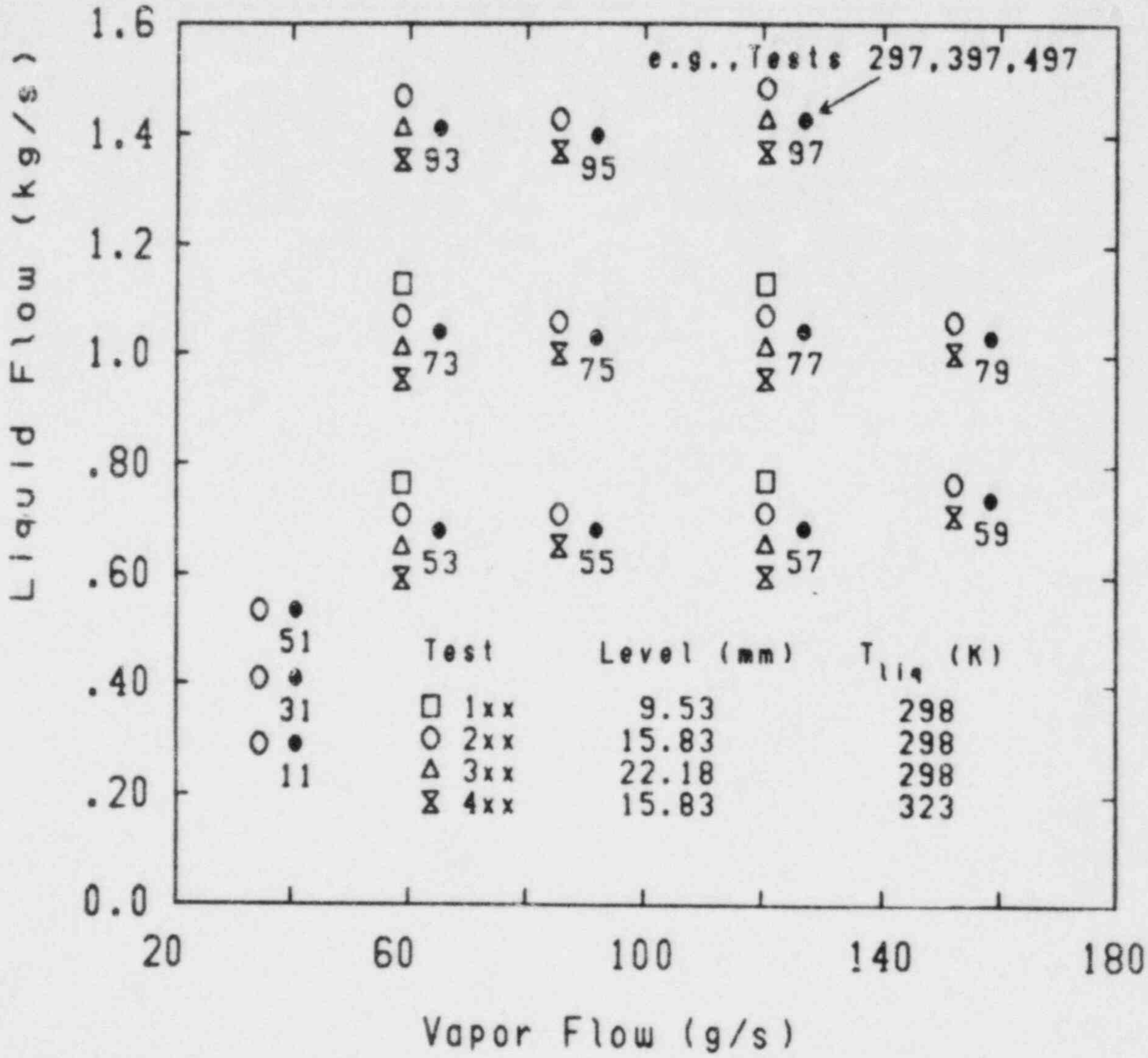

Figure 4.1 Test Configuration and Nominal Inlet Conditions for Stratified Flow Experiments

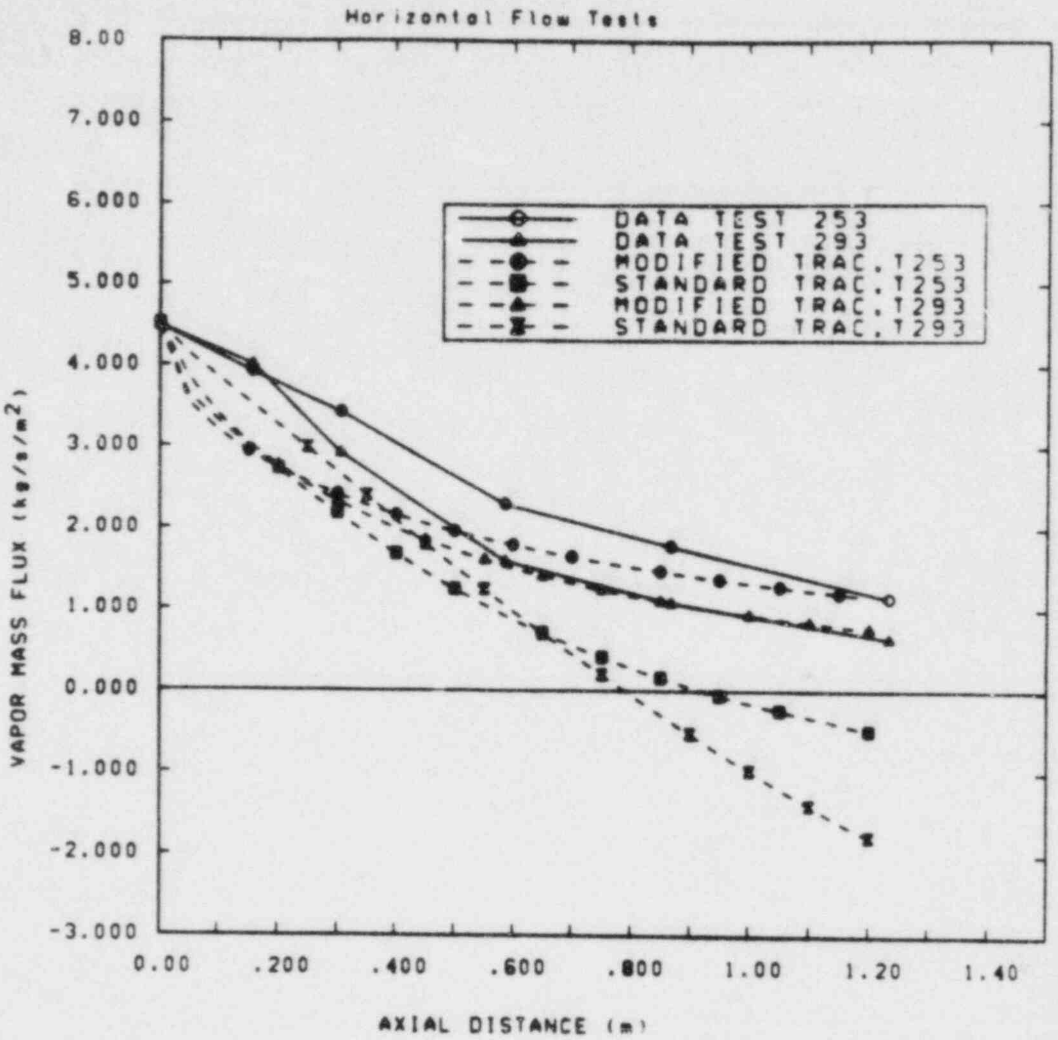

Figure 4.2 Vapor Mass Fluxes for Low Vapor Inlet Flow Cases (Tests 253 and 293)

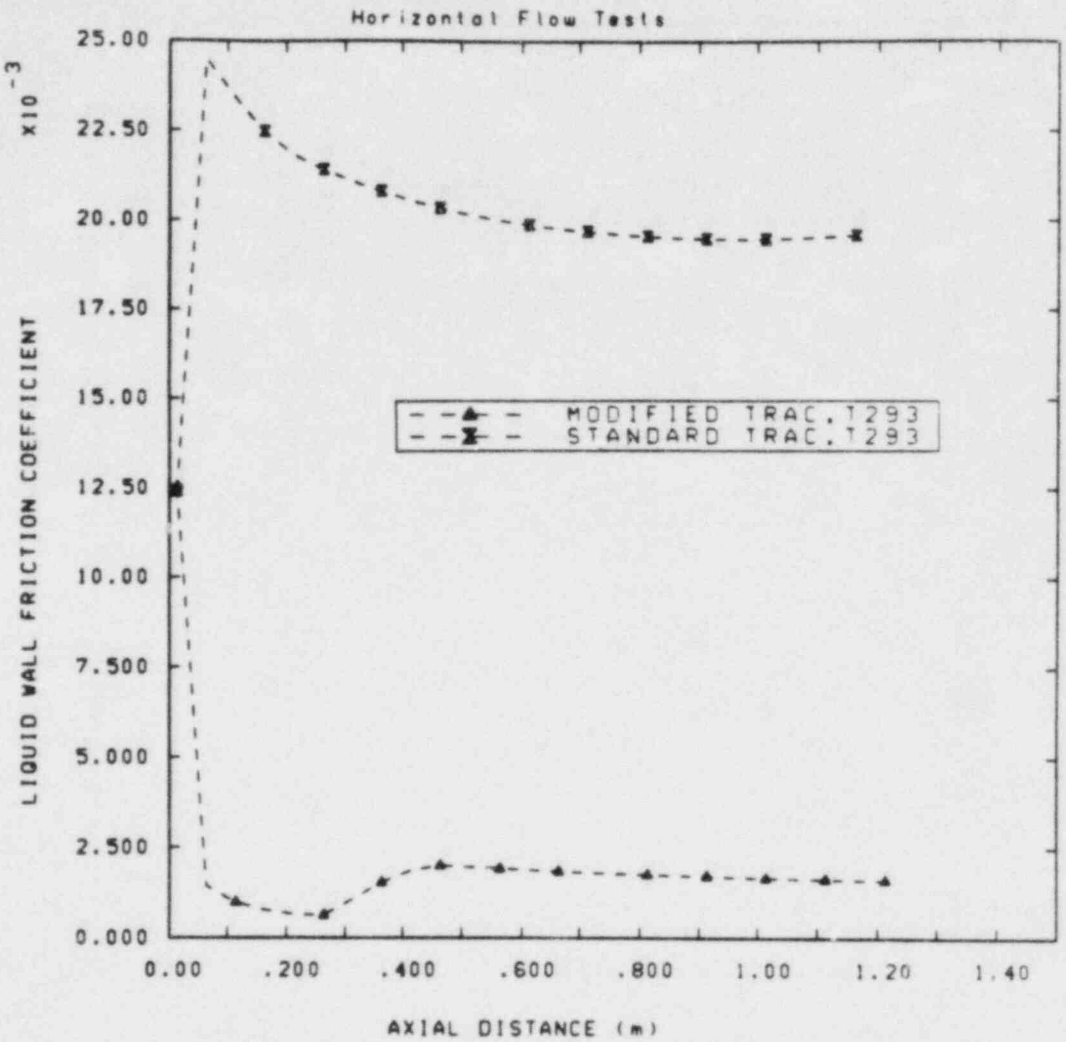

Figure 4.3 Liquid Wall Shear Coefficients for Test 293

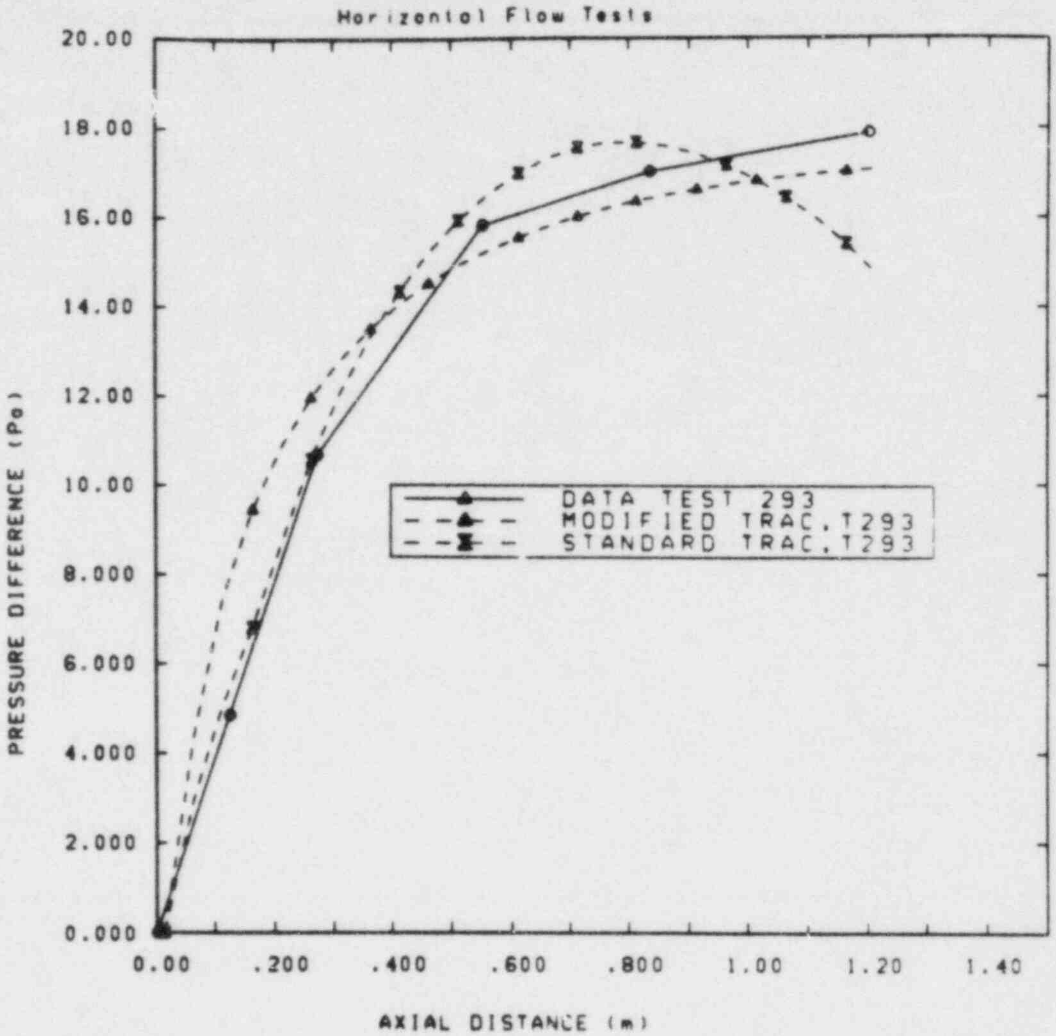

Figure 4.4 Pressure Profiles for Test 293

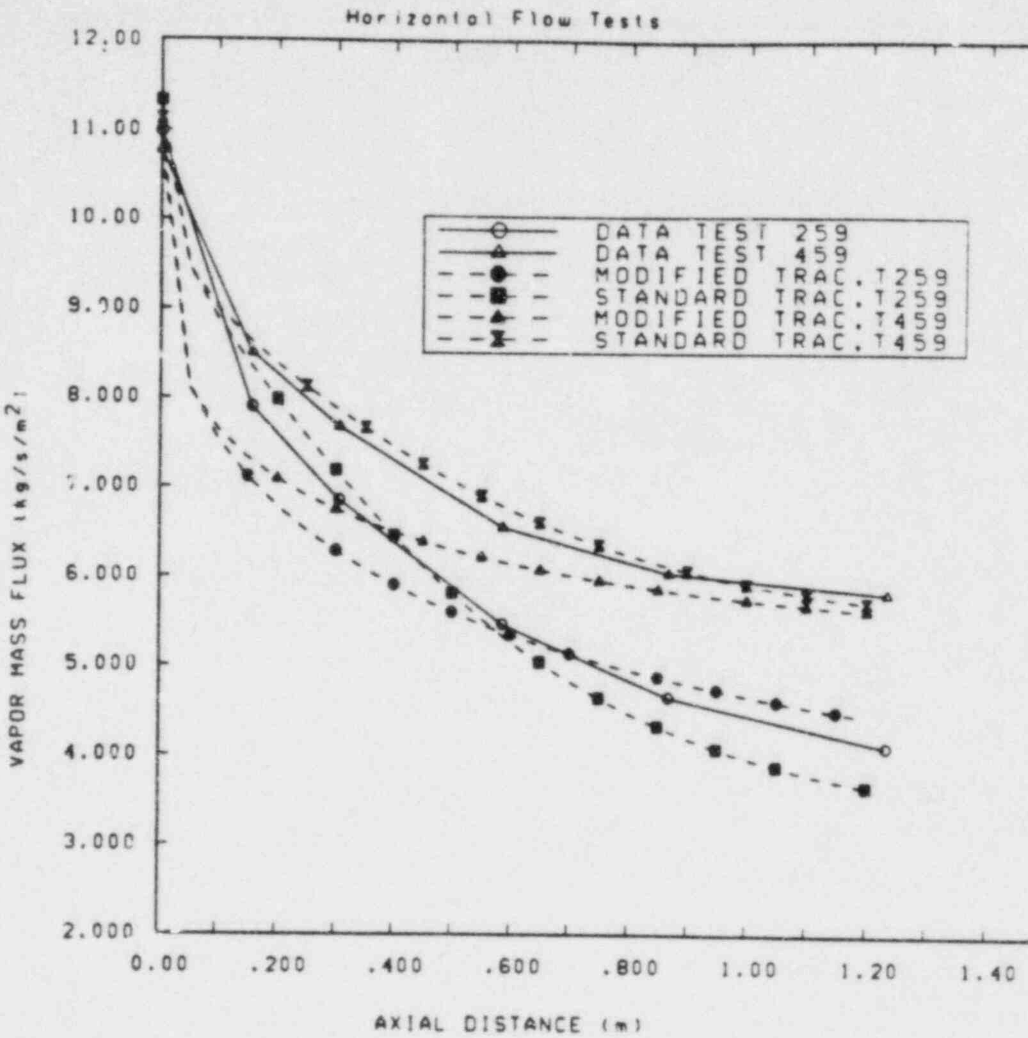

Figure 4.5 Vapor Mass Fluxes for High Vapor Inlet Flow Cases (Tests 259 and 459)

5.0 NEPTUNUS PRESSURIZER TEST

The NEPTUNUS pressurizer test facility, located at Delft University of Technology in the Netherlands, consists of a pressure vessel with a surge line at the bottom and a spray line at the top. The carbon steel test vessel is 2.5 m high and 0.8 m in diameter. The surge line nozzle diameter is 0.084 m and that of the spray nozzle is 0.027 m. Heater elements with a total power of 17 kW compensate for environmental heat losses. Test Y05 consisted of four successive insurges, combined with spray flow, and outsurges. The details of the facility and test Y05 were obtained from a RELAP5/MOD1 calculation performed by H. A. Bloemen [11].

Calculations for test Y05 using TRAC-PF1/MOD1 and 13- and 4-cell models for the pressurizer were discussed in the last quarterly. [2] Subsequent to these initial calculations, we decided that using a nodalization that included a PIPE component (so that the energy from the heaters could go directly into the coolant at the heater elevation) might be a better model. The calculations were repeated using using two different models for the test vessel. Figure 5.1 shows the new base model of the vessel, which consists of 2 PRIZER components and a PIPE component. The second model used the same geometry but with the 2 PRIZER components replaced with PIPE components. The results from both of the models were nearly identical; therefore, only the results from the base model will be discussed.

The calculated and measured pressures in the vessel are compared in Figure 5.2. The results show that the calculated pressure increases during insurges and decreases during outsurges were larger than measured. There was, however, good agreement in the minimum pressure reached during the outsurges. In the test, the rate of increase in pressure during insurges decreased quickly after the initiation of spray flow and the actual increase in pressure stopped a few seconds later; in the calculation, the pressure did not appear to stop increasing until there was a significant decrease in surge line flow.

Calculated and measured fluid and saturation temperatures are compared in Figure 5.3. Three measurements of the fluid temperature are shown and indicate some variation in the response. (The difference in the location of the measurements was not reported.) In both the test and the calculation, the vapor was superheated during insurges and saturated during outsurges. Similar to the results from the pressure comparisons, the calculated fluid temperatures were higher than measured during insurges. The calculated fluid temperature increased at a much more rapid rate than the measured temperatures, while the calculated saturation temperature changed at a rate more similar to the measured. The difference in the calculated and measured peak temperatures during flow into the pressurizer increased for each insurge. The reason for the increase in the peak temperature difference appears to be that the time between the start of the insurge until the initiation of the spray flow increased with each of the insurges. Since the calculated fluid temperature did not start to decrease until the initiation of spray flow, there was a longer time period for the temperature to increase before it was turned around by the spray flow, thus resulting in a higher calculated temperature.

The calculated interfacial and heat structure heat flow in cells 9 and 5 of component 12 (the upper PRIZER component) are shown in Figures 5.4 and 5.5, respectively. Positive values of the interfacial heat flow indicate the transfer of energy from the vapor to the liquid and negative values, from the liquid to the vapor; positive values of the slab heat flow indicate energy transfer from the fluid to the slab and negative values, from the slab to the fluid. The interfacial heat flow was mostly positive during insurges and spray flow and negative during outsurges. The slab heat flow was negative during spray flow and slightly positive during outsurges.

For both of the cells shown, the interfacial heat transfer was much larger than the heat transfer between the fluid and the vessel structures during insurges with spray flow, except during the first insurge. The heat flow at the vessel structure during insurges, when condensation was occurring on the walls, was very small (almost zero) and did not contribute significantly to decreasing the pressure. The heat flow at the slabs was nearly the same in both cells whereas, except for a brief period at 80 s in cell 9, the peak interfacial heat transfer increased from cell 9 down toward cell 5, where the highest interfacial heat transfer in the vessel was calculated.

The calculated vapor, wall and saturation temperatures for cell 9 of the upper PRIZER are shown in Figure 5.6. The difference between the vapor and saturation temperatures indicate that a significant amount of vapor superheat was calculated during the last three insurges. Examining the wall temperatures shows that, during the periods when the vapor temperature was superheated and higher than the wall temperatures and the saturation temperature was lower than the wall temperatures, the walls continued to cool down. No condensation of the superheated vapor was occurring because the system saturation temperature was lower than the wall temperature. When the system saturation temperature increased above the wall temperature, condensation occurred and the wall temperatures started to increase. The heat transfer logic in TRAC-PF1 only uses the condensation heat transfer regime when the wall temperature is lower than the saturation temperature. The initiation of spray flow and the increase of the system saturation temperature to above the wall temperature occurred at the same time; thus the effect of condensation on the system temperature response could not be identified. However, since the rate was so small it would probably not have a significant effect.

A 13-cell PRIZER model was used in the first calculation performed and reported in the last quarterly. The pressures calculated with that 13-cell PRIZER and the new base model are compared in Figure 5.7; the measured pressure is also shown for reference. This comparison shows that there was no significant difference between the results using the two models. Thus, for this test it was not important to have the energy from the heaters deposited directly into the coolant rather than through the vessel walls.

In summary, preliminary results from the comparison of pressures and fluid temperatures during insurges combined with spray flow and outsurges from a pressurizer indicate that higher maximum pressures and temperatures are calculated by TRAC-PF1/MOD1 than measured. Possible causes of these results appear to be that the interfacial heat transfer from superheated vapor to subcooled liquid was too low and that delay in condensation to the vessel walls during insurges until the saturation temperature increased above the wall temperature was too long.

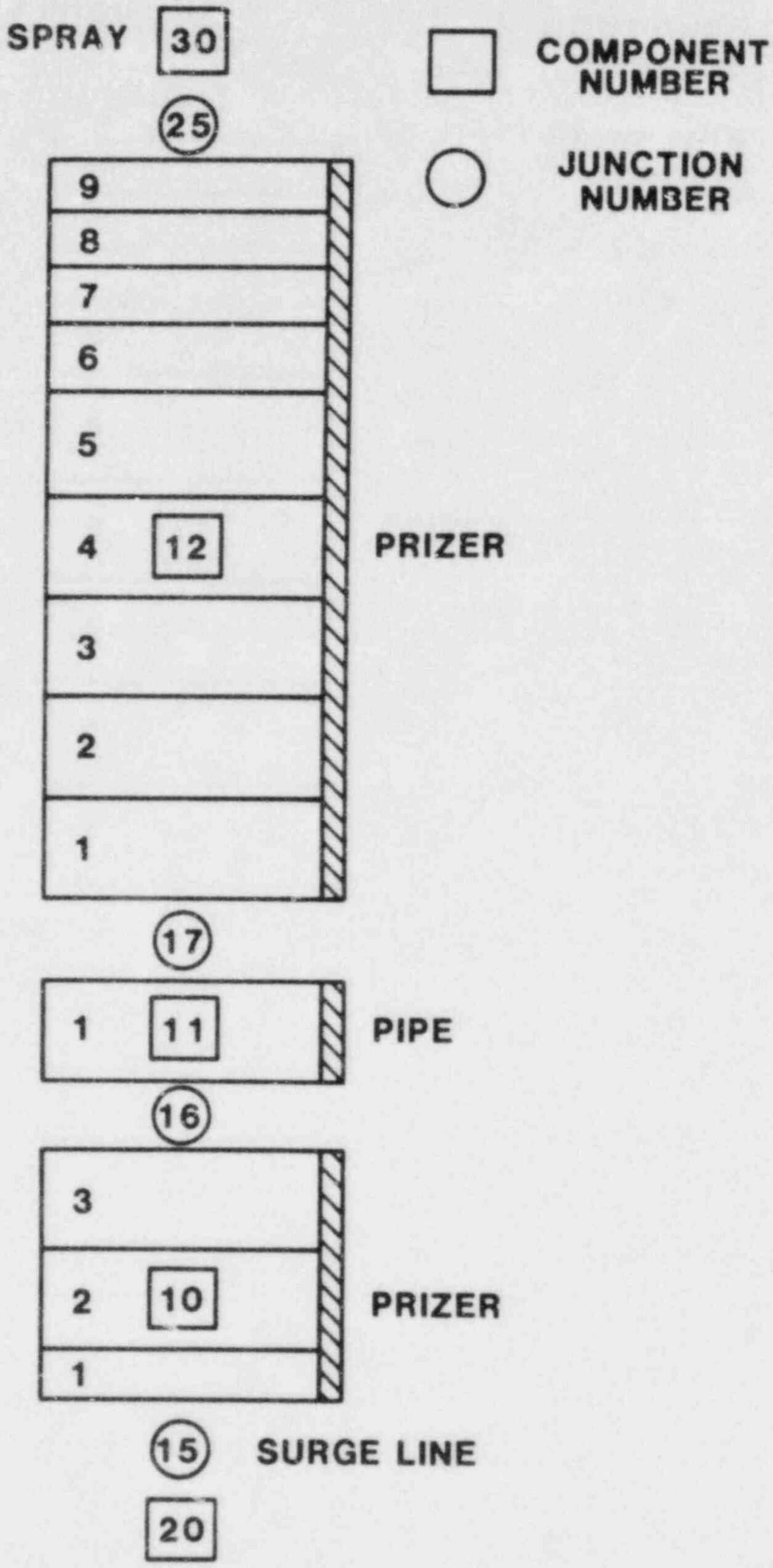

Figure 5.1 TRAC-PF1/MOD1 PRIZER/PIPE Noding Diagram for the NEPTUNUS Test Facility

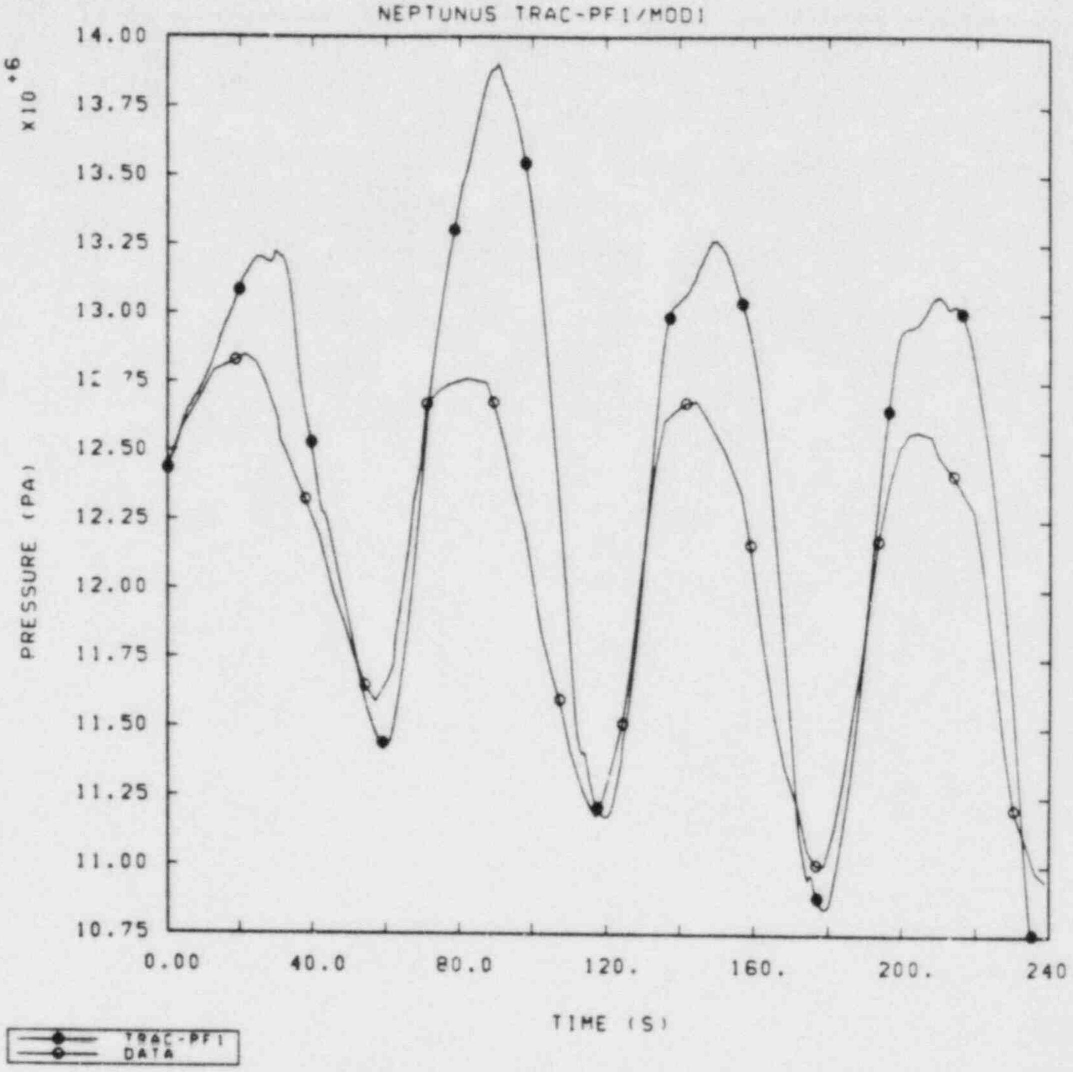

Figure 5.2 Calculated and Measured Pressures for NEPTUNUS Test Y05

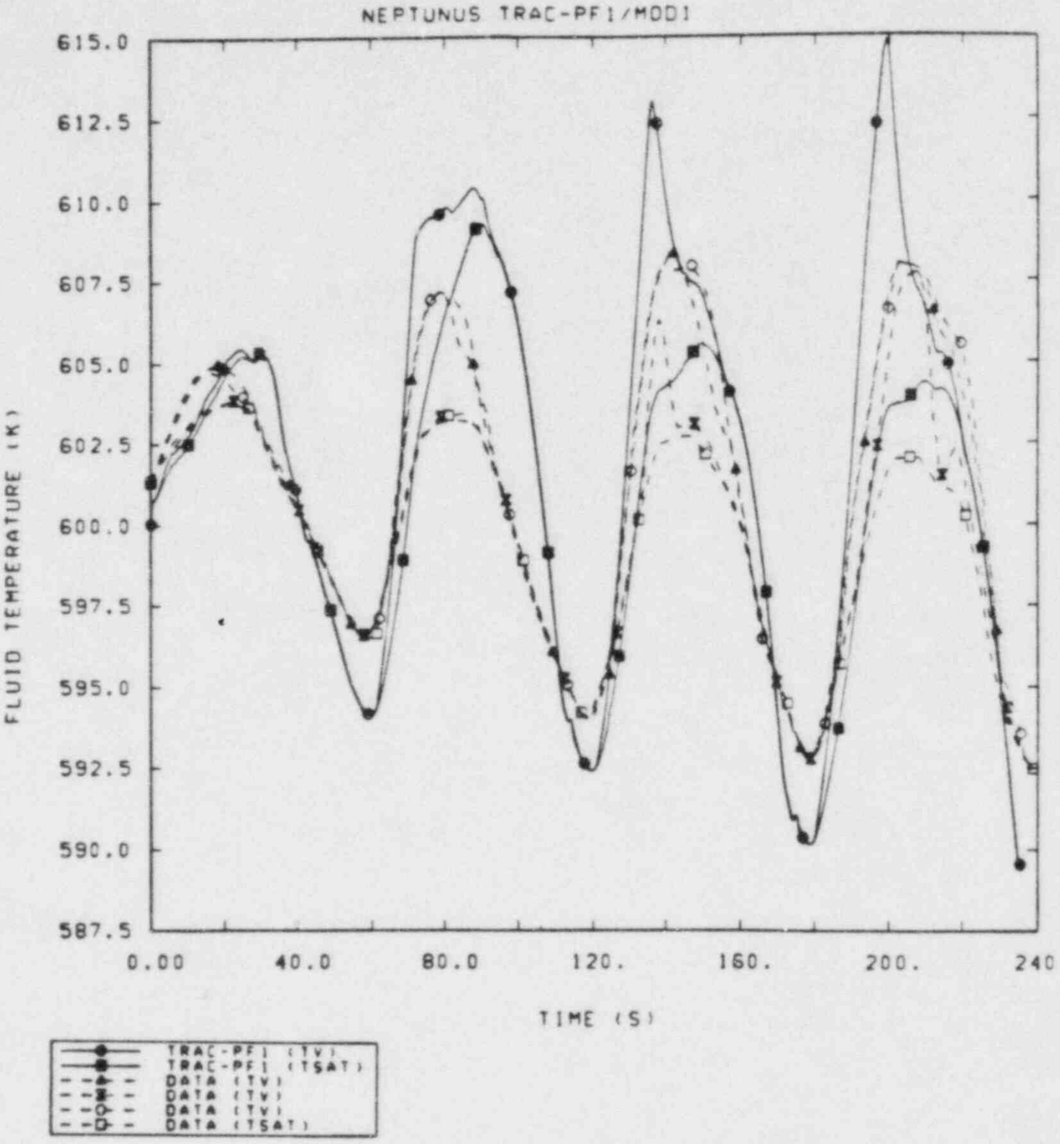

Figure 5.3 Calculated and Measured Fluid Temperatures for NEPTUNUS Test Y05

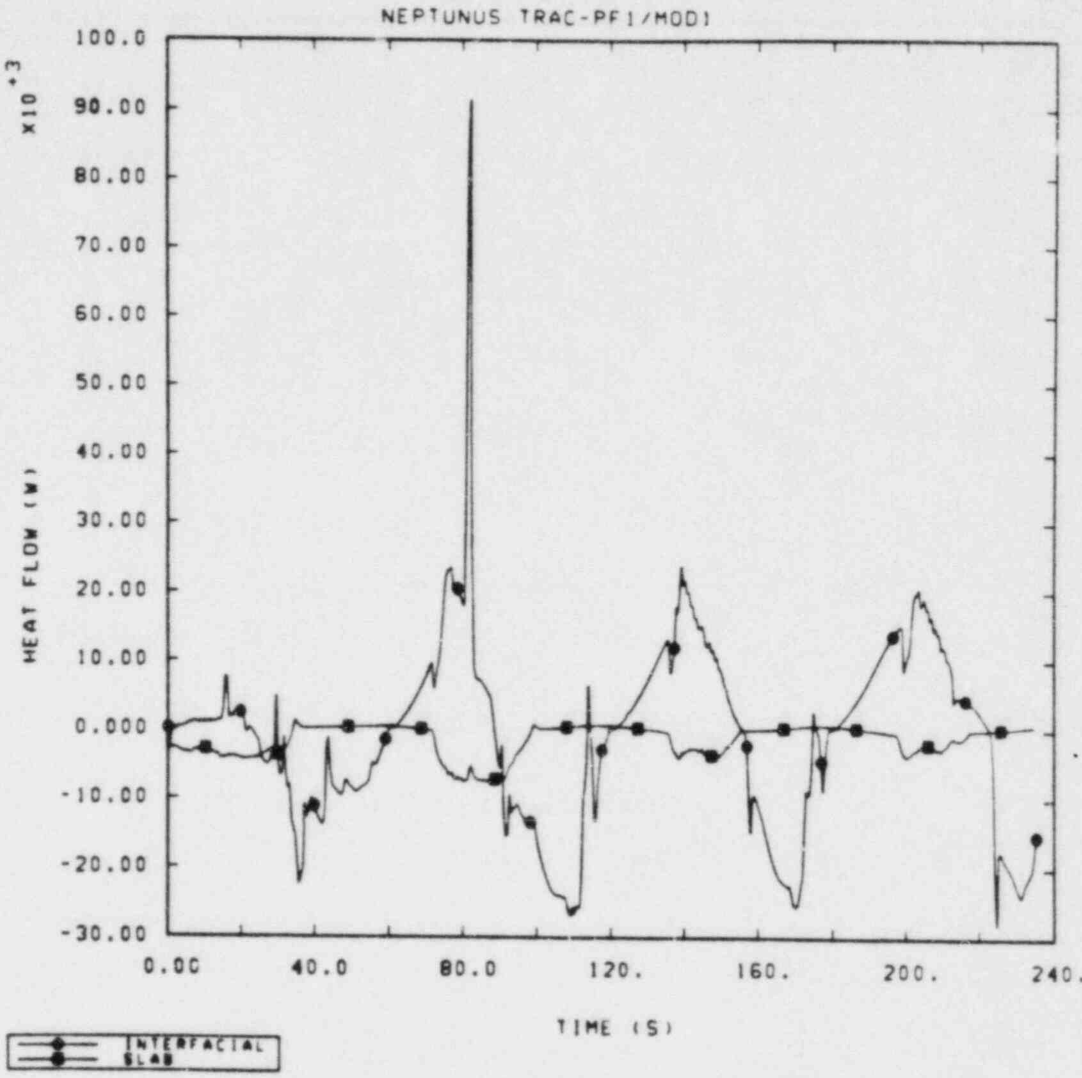

Figure 5.4 Calculated Heat Flow in Cell 9 of Upper PRIZER for NEPTUNUS Test Y05

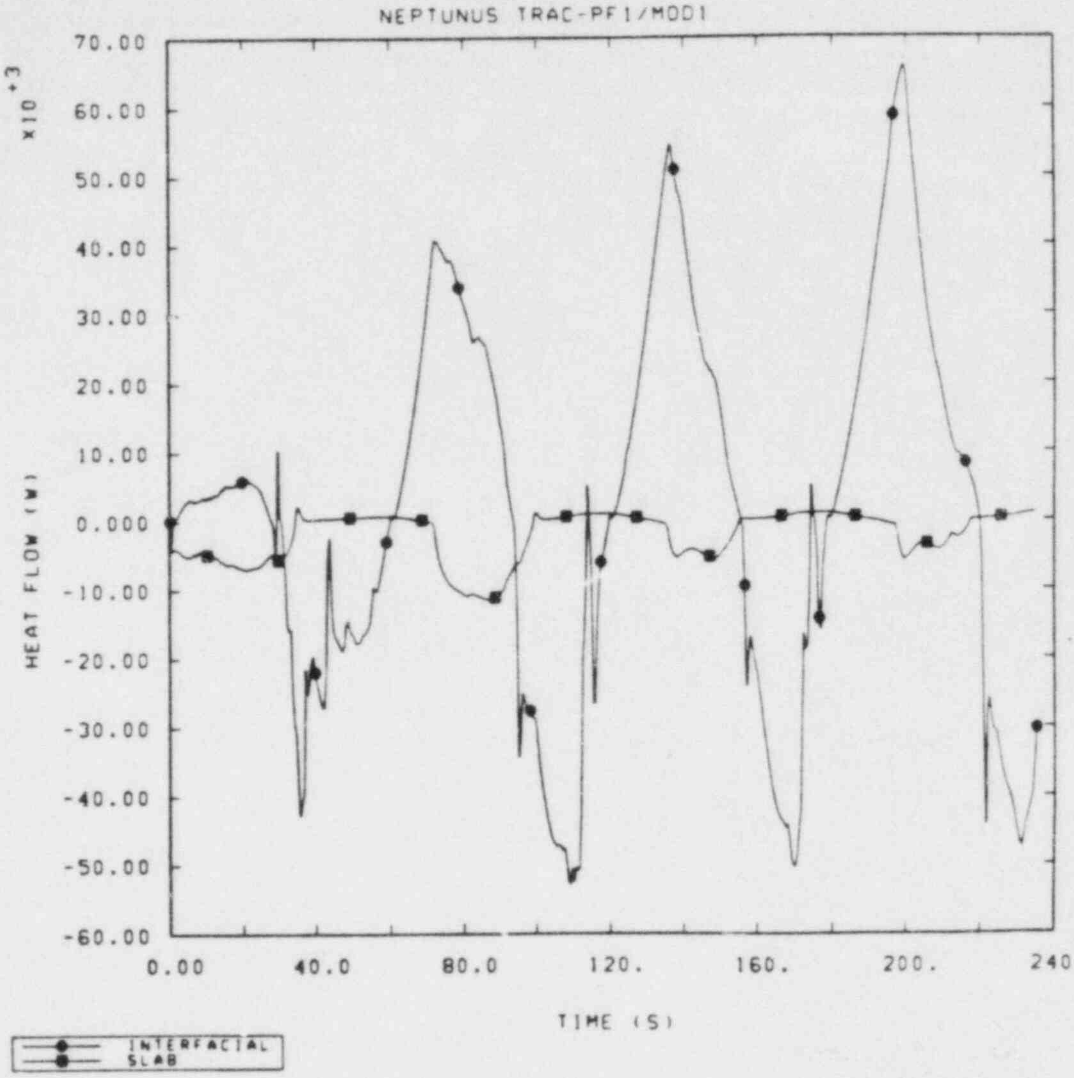

Figure 5.5 Calculated Heat Flow in Cell 5 of Upper PRIZER for NEPTUNUS Test Y05

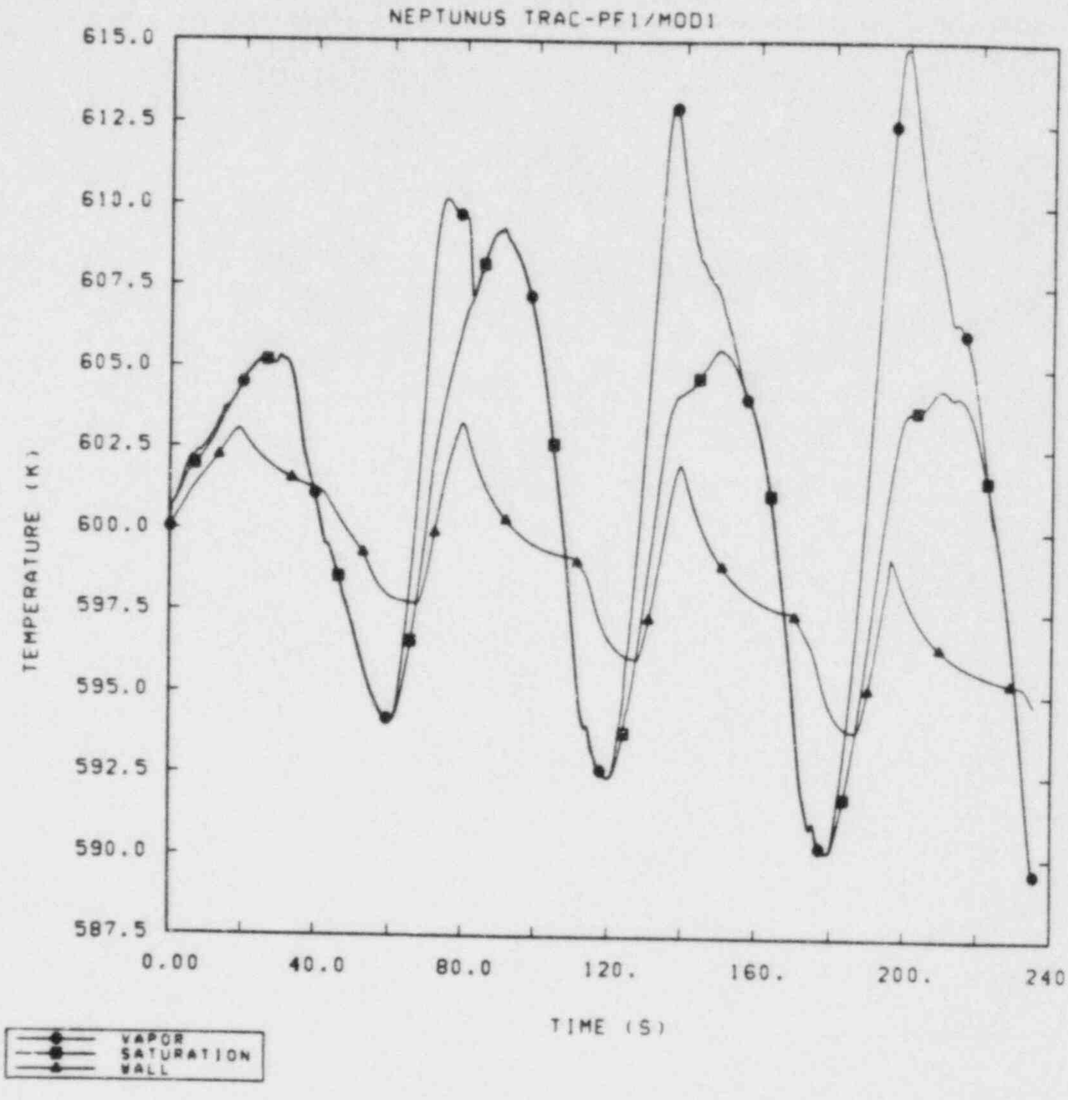

Figure 5.6 Calculated Temperatures in Cell 9 of Upper PRIZER for NEPTUNUS Test Y05

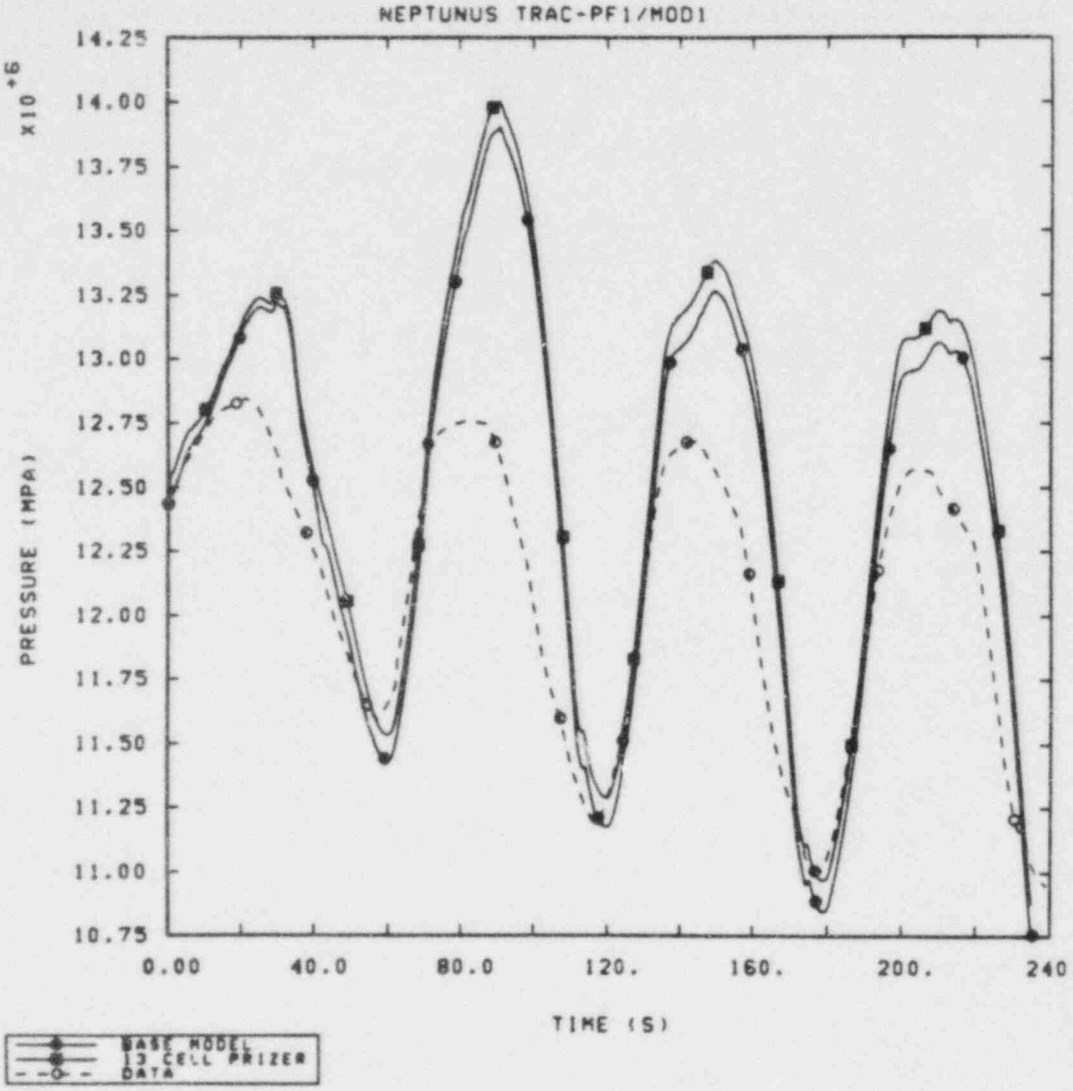

Figure 5.7 Calculated Pressures for NEPTUNUS Test Y05 using Current 13-Cell PRIZER/PIPE Model and Previous 13-Cell PRIZER Model

6.0 LOBI TESTS

The Loop Blowdown Investigations (LOBI) facility is located at Ispra, Italy, and supported by the EURATOM Joint Research Centre [12]. The facility was designed to supply experimental data on simulated LWR primary coolant system response during the initial high pressure blowdown portion of a LOCA. It is a 1/700-scale model of a four-loop 1300 MWe PWR, consisting of two primary coolant loops connected to the electrically heated reactor pressure vessel model, in which 64 rods provide a peak power of 5.3 MW. While both loops contain a fully active circulation pump and steam generator, the intact loop has three times the water volume and mass flow of the broken loop.

The two LOBI tests in our assessment matrix are A1-04R, a 200% cold leg break scenario [13,14] previously analyzed as part of our RELAP5/MOD1 assessment program [15], and B-R1M, a 25% cold leg break [16,17] which is a scaled counterpart to Semiscale intermediate break test S-IB-3 (also in our TRAC-PF1/MOD1 assessment matrix). We chose to begin work on A1-04R first, since much of the background work had already been done during our RELAP5 analyses. The steady state and transient TRAC nodalizations we developed for the LOBI facility for test A1-04R were described in the last quarterly report [3], as were the results of our A1-04R steady state analyses.

6.1 A1-04R Large Break Test

At the start of this quarter, we ran a calculation for large break test A1-04R for almost 70 seconds of transient (with 10 seconds of steady state preceding for plot purposes), using version 11.1 of TRAC-PF1/MOD1. The calculated pressures and break flows are in reasonably good agreement with data, using the same values for the discharge coefficients as in the earlier RELAP5/MOD1 analyses (i.e., 1.0 for subcooled flow and 0.85 for saturated flow). The calculated peak clad temperature, however, was significantly higher (~40 K) than the measured value; the total core rewet at 5-15 seconds was not calculated at all (except at the very top of the core); and the code results showed no signs of a quench front moving up the core at late times, although the data shows the middle core quenching from 25 to 55 seconds.

Studying these results and those of the B-R1M transient calculations discussed below, we found and corrected a number of input errors in our LOBI A1-04R and B-R1M decks. The major impact on the A1-04R large break analysis came from correcting the power shape input to a power density shape input, which resulted in a calculated peak clad temperature in excellent agreement with data, within 1 K of the measured value. With the early-time core response thus in much better agreement with data, we then searched for possible causes of not calculating the observed total core rewet at 5-15 seconds; we feel that missing this rewet may be largely responsible for the lack of a calculated core quench later in the transient, since without this rewet the rods in the calculation are significantly hotter late in the transient compared to data.

The core rewet occurs in the test because the onset of flashing in the over-scaled vessel downcomer temporarily reestablishes positive core flow and pulls a slug of liquid from the lower plenum up through the core and out the hot legs. The calculation showed a liquid slug entering the core, but then dissipating as it moved up and totally missing in the hot leg density plots; hand estimates seemed to indicate that this slug should be able to cool the rods more than it did in the calculation.

At the time, a possible cause of not calculating the observed total core rewet at 5-15 seconds in our A1-04R large break transient analysis appeared to be the prediction of substantial (~10 K) liquid superheat in much of this liquid slug during the relevant 10 second period. The liquid can retain this unphysical degree of superheat because the interfacial area term (ALV) for interphase heat transfer was identically zero. After a number of discussions with the code developers (in particular, John Mahaffy), LANL identified a coding error in the 3-D constitutive package; with this error corrected, no spurious liquid superheat is calculated.

Because a number of other errors are known and have been fixed, we reran this A1-04R calculation with version 11.6 late in June, up to the time accumulator injection begins (which occurred in the calculation within 2 seconds of the time measured). Despite the numerous code changes, the overall results were very little different from those calculated previously with version 11.1. No core rewet was calculated at 5-15 seconds, and the late-time rod temperatures were much higher (~150 K) than measured. These late-time temperatures were found to be very sensitive to the discharge coefficients used; changing the saturated discharge coefficient from 0.85 to 1.0 (which gave better agreement on the time accumulator injection started) increased the late-time rod temperatures by ~90 K.

6.2 B-R1M Intermediate Break Test

During this quarter, we modified the A1-04R input deck to use the B-R1M intermediate break test boundary conditions and completed a B-R1M steady state calculation. We then ran the first part (~50 seconds) of the B-R1M intermediate break transient with version 11.1. Results from our initial calculations showed the primary system depressurizing much slower than measured.

Searching for likely causes of this discrepancy, we found several input errors, notably in the pressurizer volume and surge line resistance. Correcting these resulted in better agreement with data, but the calculated depressurization was still slow.

We included the pump seal leakage in the model, and recalculated the secondary side steady states for both steam generators, since examination showed the steam generators in the first analyses running at very low secondary side liquid inventories. The "corrected" steam generator secondary side steady states had liquid inventories very similar to those in our earlier RELAP5/MOD1 LOBI analyses, since no experimental data on secondary inventories were given. With these corrections, we reran the first ~50 seconds of the B-R1M intermediate break transient (still with 11.1). The results were similar to those from our earlier runs, with the primary system depressurizing more slowly than measured. However, further analysis shows the calculated pressure and core rod temperatures higher than data, but calculated intact and broken loop hot and cold leg temperatures lower than data, which is contradictory.

Later this quarter, we reran the B-R1M transient with version 11.6, up to the time accumulator injection begins (which is calculated to occur within 6 seconds of the observed time, in a 300-second transient). Again, no big differences were seen from the previous 11.1 results. The calculated primary pressure was higher than measured for about 70 s; however, the calculated pressure then dropped more rapidly than observed, so that the accumulator setpoint pressure was reached at about the right time. There are some differences between calculated results and data (such as going into reverse heat transfer later in the calculation and not predicting some partial clearing of the intact loop pump suction before the final complete clearing), but generally the agreement is very good.

7.0 SEMISCALE TESTS

The Semiscale Mod-2A test facility is located at the Idaho NAtional Engineering Laboratory and supported by the NRC. This scaled integral facility is used to investigate the thermal and hydraulic phenomena accompanying various hypothesized loss-of-coolant accidents and operational transients in a PWR system. It is a 2/3411-scale model of a four-loop PWR, consisting of two primary coolant loops and external downcomer connected to an electrically-heated reactor pressure vessel model, in which 25 rods provide a peak power of 2.0 MW. While both loops contain a fully active circulation pump and steam generator, the intact loop has three times the water volume and mass flow of the broken loop.

Of the three Semiscale Mod-2A tests in our TRAC-PF1/MOD1 assessment matrix, we chose to start with the intermediate break test S-IB-3 [18,19,20]. This test was designed to duplicate as closely as possible the LOBI B-R1M test, which is also in our assessment matrix. The LOBI B-R1M test was a 25% break in the LOBI facility which, when area-to-volume scaled to the Semiscale facility, resulted in a 21.7% break test in the Semiscale facility; both tests simulate cold leg break LOCAs. The deck developed for S-IB-3 is now being modified for the S-SF-3 main feedline break transient [21,22,23], the next test we are analyzing.

7.1 S-IB-3 Intermediate Break Test

The TRAC-PF1/MOD1 nodalization we developed for test S-IB-3 in the Semiscale Mod-2A facility was described in the last quarterly [3]; this S-IB-3 deck has now been modified to include the required steady state boundary conditions and pump speed controllers, and steady state analyses were completed this quarter.

We have done a number of steady state calculations for this intermediate break test, with the final results given in Table 7.1.1. The resulting primary side conditions are in reasonably good agreement with data, except for the broken loop pump speed (which was expected), and the intact and broken loop cold leg temperatures (which are too high for given secondary side conditions even with the minimum tube-to-tube spacing used as the heated equivalent diameter). Based primarily upon the results of our LOBI B-R1M analyses, we have taken care to ensure a good secondary side steady state before beginning any transient analyses.

The first S-IB-3 steady state results had too much secondary side liquid inventory in both steam generators, and the feedwater flows were much higher than needed to remove the core power (with most of the feedwater being entrained and swept out the steam outlet without participating in the heat transfer processes). We have rerun the steady state with feedwater flow controllers referencing the secondary side liquid level (developed for the S-SF-3 steady state, as discussed below) and with a "separator K" to ensure pure steam outflow.

For these reruns, the steam generators were first run as "stand-alone" problems to test various control strategies and boundary conditions. In these stand-alone problems, the feedwater was first reduced and the secondary inventory allowed to boil off until it was substantially below the desired experimental value. A steam-separator K of 1.0E30 was then put in at the model junction corresponding to the actual location of the steam separator, and the feedwater was controlled to achieve a specified downcomer collapsed liquid level without overshooting the desired conditions. This technique was eventually successful for both steam generators, but with two problems encountered; one was an input error we could correct, but the other was a code difficulty we could only hope to avoid.

The input error lay in assuming the collapsed liquid level control function was a cell-centered variable so that the ordering of the component cells to be included did not matter. In fact, this variable is referenced to particular cell edges and the ordering is important (and was originally wrong). With the wrong liquid level driving the feedwater controller, a number of odd results were calculated.

The error in liquid level definition resulted in a signal variable value lower than the actual liquid level being calculated. As the feedwater controller then tried to increase this liquid level, the actual level approached the downcomer/separator junction and the calculation would often predict rising pressures until a steam table failure occurred. The perfect separator in TRAC has difficulty relieving steam generator overpressuriztion due to excess liquid inventory because it can only pass vapor.

With careful adjustments in the controller constants (based on the experience gained in the S-SF-3 steam generator steady state calculations described below), the correct secondary side steady state conditions were eventually calculated. The EXTRACT utility program was then used to insert these conditions in the overall S-IB-3 deck, and the system steady state was then successfully run. The few modifications required for the S-IB-3 transient, such as modelling the break valve assemblies, the steam generator isolation, and the pump and core power ramps, will be made next quarter and the transient calculation will be begun.

Table 7.1.1 Semiscale S-IB-3 Initial Conditions

Parameter	Data	Calculation
Core Power (MW)	1.451	1.451
System Pressure (MPa)	15.53	15.53
IL Cold Leg Temperature (K)	560	565
BL Cold Leg Temperature (K)	566	571
IL ΔT (K)	36	30
BL ΔT (K)	31	25
IL Cold Leg Flow (kg/s)	6.18 (8.02 ℓ/s)	6.18
BL Cold Leg Flow (kg/s)	2.13 (2.74 ℓ/s)	2.13
IL Pump Speed (rad/s)	177	178
BL Pump Speed (rad/s)	872	1281
SG Feedwater Temperature (K)	494	494
IL SG Pressure (MPa)	6.48	6.30
BL SG Pressure (MPa)	7.53	7.40
IL SG Liquid Level (m)	7.327	~7.3*
BL SG Liquid Level (m)	7.138	~7.1*

* Slow oscillations of ~0.1 m present in calculation

7.2 S-SF-3 Feedline Break Test

Work on the TRAC assessment calculations for two tests in the Semiscale SF series began this quarter. After the available documentation on feedwater line break test S-SF-3 [21,22,23] was reviewed, our S-IB-3 input deck was modified for the S-SF-3 conditions; the modifications required are minor, since the S-SF test series was run in the same Semiscale Mod-2A facility as the S-IB series. The 3-D VESSEL used for S-IB-3 will later be converted to a 1-D CORE model with associated 1-D piping for the rest of the vessel, after a satisfactory steady state has been achieved. A component schematic for the Semiscale Mod-2A system during these S-SF tests is given in Figure 7.2.1.

The necessary input changes included modifications to the steam generator secondary sides and addition of control and trip logic peculiar to feedwater line breaks. The major change made to the secondary sides was the addition of a TEE to allow injection of feedwater at the bottom of the downcomer, instead of at the top (with the old injection location at the top of the downcomer still used for aux feed injection). The piping necessary to initiate the feedwater line break and to allow isolation of the secondary sides was also added. The annular flow friction factor option was used in the downcomer and the homogeneous flow friction factor option was used in the boiler region.

Form loss coefficients (K factors) were added to model the effects of the tube support plates on the secondary side, as opposed to using the automatic form loss calculation provided in TRAC with the reduced vena contracta area input. That abrupt area change model would have required using two cells per baffle plate in the boiler region and corresponding doublings in the U-tube primary cells and in the downcomer region noding, increasing the number of cells in each steam generator by ~40 and also increasing the number of heat slabs in each generator by ~60, which we considered unacceptable. This use of K factors and choice of friction factor options was based on our experience with modelling the B&W once-through steam generator (OTSG) tests [4] using TRAC-PF1/MOD1.

Another modification of interest was the addition of a leakage path from the primary side. This path was modelled using two TEE components located at the bottom of the intact loop pump suction. A BREAK component was attached to the side tube of one TEE and a FILL component was attached to the other. A K factor (determined by trial and error) was added to the junction adjacent to the BREAK to achieve the reported steady state leakage rate; the FILL component was used to provide the necessary makeup flow. During the transient the makeup supply will be terminated, as was done in the experiment. We felt that this modification might be important because the leakage rate is of the same order of magnitude as the HPI flow during the transient.

Control logic was added to adjust the pump speeds to achieve the reported loop flow rates. Also, a control block to adjust the feedwater flow to achieve the reported secondary side inventory was added. The control logic for both the pump speeds and the feedwater flows is of the form

$$PNEW = POLD\ [cR + (1-c)]$$

where PNEW is the new value of the parameter being adjusted, POLD the value of the parameter at the previous time step, c is an arbitrary constant (0.2 for the pump speed controller and 0.5 for the feedwater controller), and R is the ratio of the desired-to-actual control block input (pump speed for pump controller and steam generator secondary side inventory or water level for the feedwater controller). The value of c and the control block minimum and maximum limits are adjusted on a trial and error basis to prevent over- or under-control, which could lead in turn to undesired oscillations.

We have encountered considerable difficulties while attempting to achieve the reported steady state conditions, particularly on the secondary side. The major difficulties involve the modelling of the steam separator located in the steam dome. (This is a mechanical separation device that employs swirl vanes to remove liquid drops from the exiting vapor.) We found that, if the separator is not modelled, the feedwater must be increased by over a factor of three to compensate for the considerable amount of liquid being entrained by the exiting vapor in the calculation; this was done by the feedwater control block which was set up to maintain the reported secondary side inventory. Although the feedwater flow is too high, the remaining steady state conditions on both the secondary and primary sides are in fairly good agreement with experimental data.

The secondary side exit vapor, liquid and total mass flows for this case (no separator model) are shown in Figure 7.2.2. About 70% of the intact loop power load is removed by generation of vapor which exits the steam dome at a rate of about 0.7 kg/s. The remaining 30% of the power load is removed by the heating of the liquid to saturation temperature. However, while a steady state can be achieved if the separator is not modelled, it would be preferable to implicitly model the separator and thereby allow injection of feedwater at the correct rate. The distribution of the secondary side fluid should also be more representative of the experiment if the separator is modelled.

A separate TRAC input model was then prepared which contained only the intact loop steam generator with appropriate boundary conditions. (This was done to allow easier and quicker investigation of the steam separators and feedwater flow.) A number of calculations were then performed using this "stand-alone" steam generator model.

The method available in TRAC to model the separator involves the input of a K factor greater than 1.0E24 at the desired cell edge. This triggers specific logic in TRAC that sets the liquid friction factor equal to the input K factor (essentially infinite liquid friction) and also sets the interfacial friction to zero. Use of this option was not successful at first. The cell immediately below the separator filled as the entrained liquid was separated from the exiting vapor. The exit vapor flow, therefore, decreased to zero while vapor generation in the boiler continued. As a result, the cell pressure increased to the limit of TRAC's thermodynamic properties routines, as demonstrated in Figure 7.2.3. To prevent this unwanted pressure increase, the accumulated liquid must be removed from the cell via the downcomer. Unfortunately, the liquid would not naturally flow into the downcomer fast enough.

Several attempts to correct this difficulty were made, including moving the location of the separator, making the downcomer connection pipe vertical, and adjusting the initial conditions and control block parameters in an attempt to "creep up" on the desired conditions. Moving the separator location to the top of the cell adjacent to the downcomer connection and making the downcomer connection pipe vertical improved downcomer flow, but were not sufficient to solve the problem. After much effort, the desired steady state conditions on the secondary side were achieved by carefully adjusting the control block parameters and initial conditions. We found that, when using the controller as described above, it was necessary to set the upper limit for feedwater flow only slightly higher than the desired flow to prevent overshooting the desired inventory. It was also necessary to use an initial inventory less than the desired inventory and to allow the feedwater controller to increase the feedwater flow. The response was very sensitive to any changes made by the controller and it took a great deal of trial and error to find the appropriate control block parameters and initial conditions. Perhaps a more sophisticated controller could be developed to reduce the controller sensitivity, but this will be attempted only if further problems with the separator are encountered.

The feedwater flow and steamline flow are plotted on Figure 7.2.4 for the "steam generator alone" case using the separator model. The small fluctuations in feedwater flow are a result of the controller action to adjust the inventory. The steamline flow exhibits sharp periodic fluctuations. The use of a separator K appears to introduce this oscillatory behavior; however, the average exit flow is correct. The inventory, shown in Figure 7.2.5, slowly converges to the desired value of 114.7 kg. The flow into the downcomer is shown in Figure 7.2.6. This quantity was not measured during the experiment, but represents the amount of liquid separated from the exiting vapor and recirculating through the steam generator.

A separate input model for the broken loop steam generator was also constructed, and the above procedure of adjusting the initial conditions and control block parameters was repeated. Additional difficulties were encountered with the broken loop, using the procedures and controllers that had given the correct steady state for the intact loop. Although the desired inventory was achieved, the secondary side pressure increased to about 7.0 MPa, instead of the desired 6.46 MPa, as shown in Figure 7.2.7. Lowering the desired inventory from 126 kg to 112 kg, in an effort to get the liquid level farther away from the separator, did not alleviate the problem. However, moving the separator to the exit of the steam generator and decreasing the exit pressure boundary condition to 5.7 MPa resulted in calculation of the correct secondary side pressure below the separator. We do not understand why such a large pressure drop occurs across the separator for the broken loop steam generator.

Unfortunately, when this separate steam generator model was included in the full system, it did not behave in the same way and a steady state could not be achieved. Addition of a controller to adjust the exit pressure to achieve the desired steam dome pressure was also unsuccessful.

An alternate method of modelling the separator was then attempted. This method does not use the large separator K but instead involves the use of a very large flow area at the steam dome exit; the large area has the effect of reducing the exit vapor flow such that the amount of entrained liquid is decreased to essentially zero. If the area was made too large, difficulties in the numerics caused the code to fail. If the area was too small, insufficient separation occurred. However, an area 50 times larger than the physical area was found to work well. In fact, this separator model worked much more smoothly than the separator K model in conjunction with the feedwater controller. The independent steam generator model ran about 30% faster when using the increased area than when using the separator K.

The full facility steady state calculation was repeated using this increased flow area separator model on the broken loop and the separator K model on the intact loop. The reported steady state conditions for S-SF-3 are given in Table 7.2.1 along with the calculated results with and without a separator model on the secondary sides. This table shows that relatively good agreement with data is being achieved. Multiplying the reported loop mass flow by the enthalpy difference from cold leg to hot leg at the reported temperatures yields a power level of about 2.1 MW; this is inconsistent with the reported power level of 2.0 MW. However, the uncertainty associated with the temperature readings is $\pm$1 K and the uncertainty in the mass flow is approximately 0.4 kg/s. The flows in the TRAC calculation are being set by a controller to exactly equal the reported mass flow. Therefore, the uncertainty associated with the flow will be reflected in the loop ΔTs. This gives an effective loop ΔT uncertainty of about 4 K and the calculated ΔTs are within this range of uncertainty.

Table 7.2.1 Semiscale S-SF-3 Steady State Initial Conditions

Parameter	Reported	Calculated	
		No Separator	Separator
Core Power (MW)	2.0	2.0	2.0
Pressurizer Pressure (MPa)	15.13	15.13	15.13
IL Cold Leg Temperature (K)	563.0	569.2	569.6
BL Cold Leg Temperature (K)	561.5	565.9	566.6
IL ΔT (K)	35.1	31.3	31.3
BL ΔT (K)	37.2	33.7	33.6
IL Cold Leg Flow (kg/s)	8.45	8.45	8.45
BL Cold Leg Flow (kg/s)	2.16	2.16	2.16
IL Pump Speed (rad/s)	244	244.7	244.7
BL Pump Speed (rad/s)	1010	1314.0	1316.0
IL Secondary Pressure (MPa)	6.31	6.31	6.31
BL Secondary Pressure (MPa)	6.46	6.46	6.46
IL Secondary Inventory (kg)	114.7	114.6	115.0
BL Secondary Inventory (kg)	126.4	125.6	126.9
IL Feedwater Flow (kg/s)	1.0	3.9	0.96
BL Feedwater Flow (kg/s)	0.25	1.3	0.25

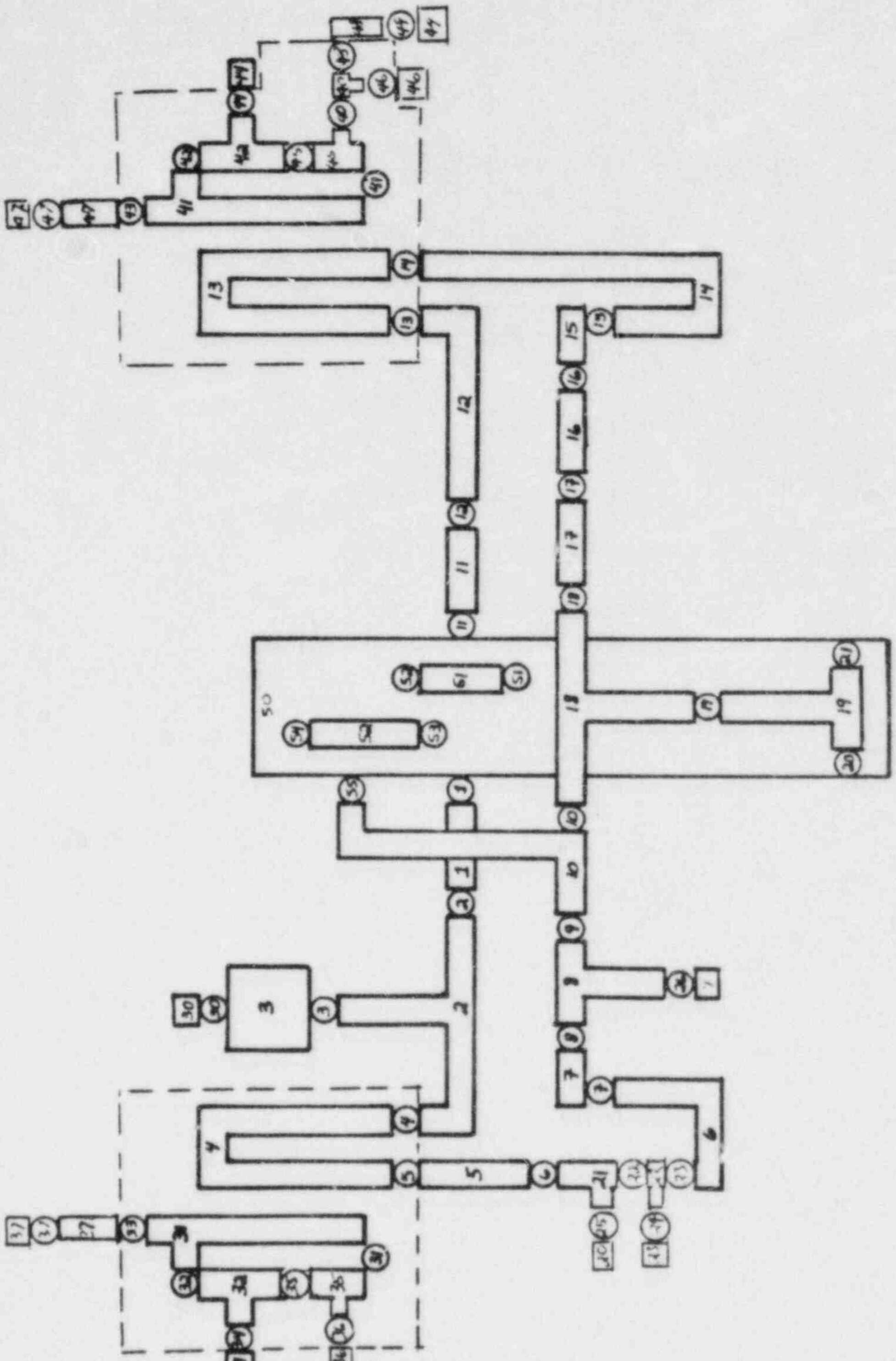

Figure 7.2.1 Preliminary Nodalization for Semiscale Test S-SF-3

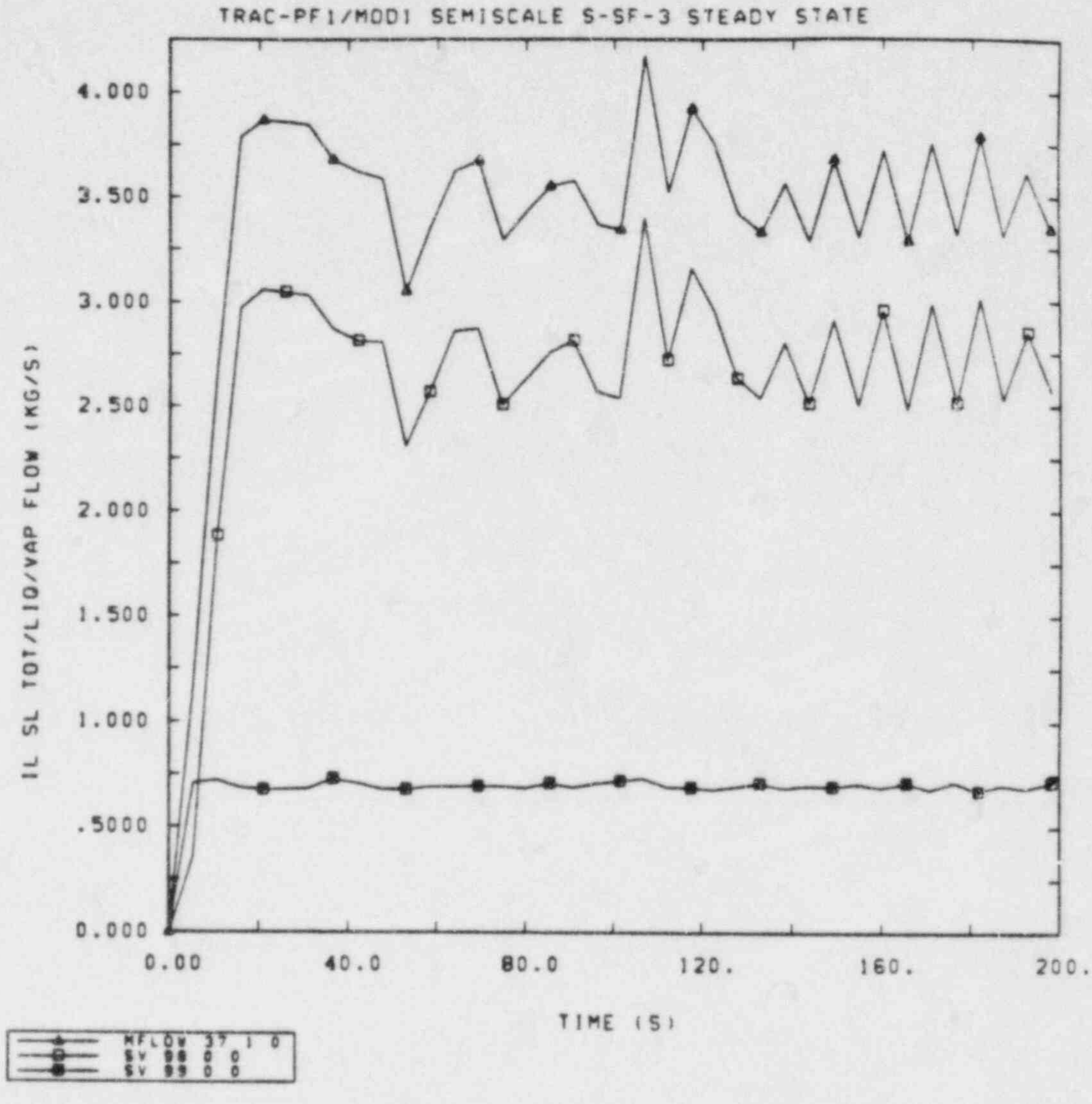

Figure 7.2.2 Total, Liquid and Vapor Flows for Intact Loop Secondary Side Steam Generator Exit

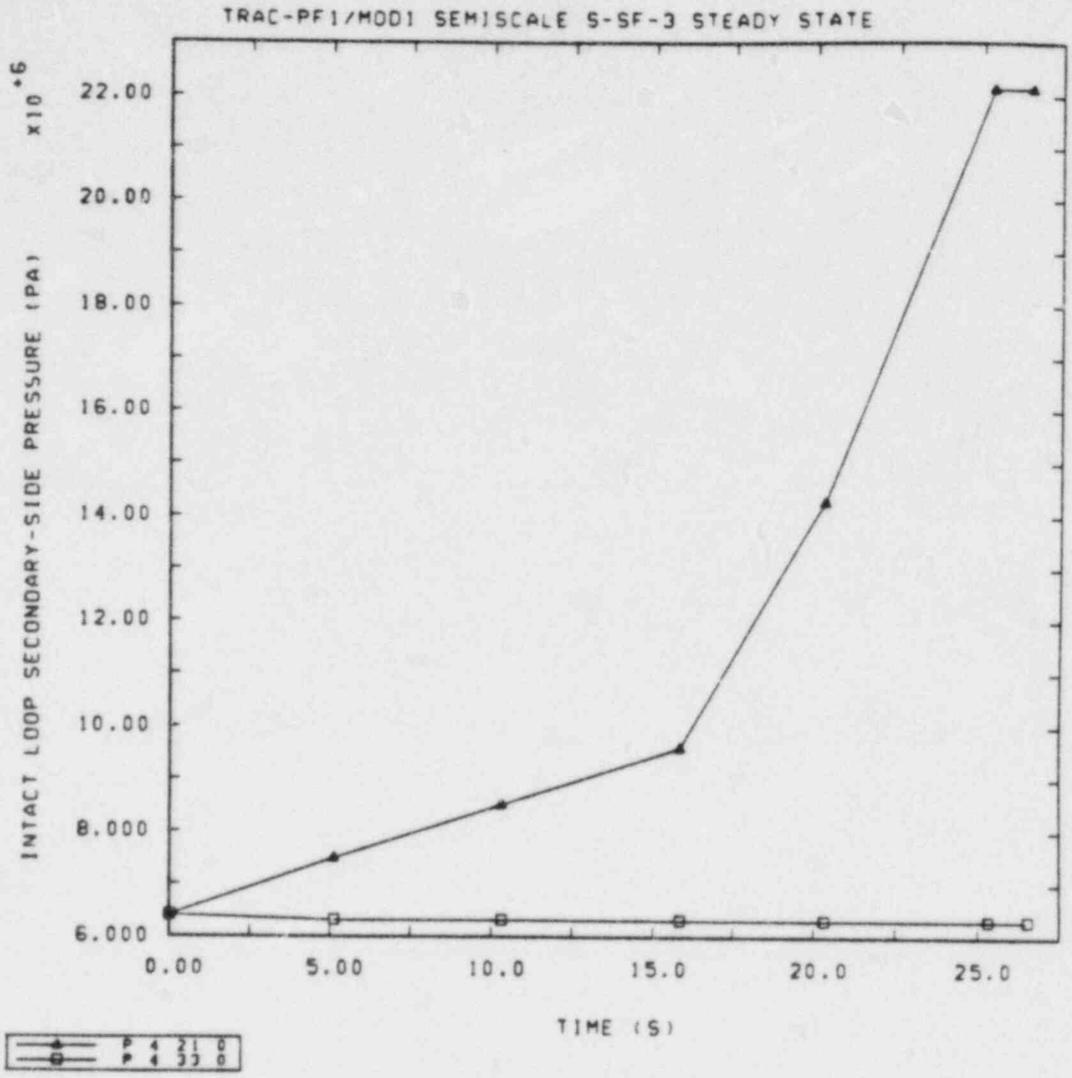

Figure 7.2.3 Intact Loop Secondary Side Pressure

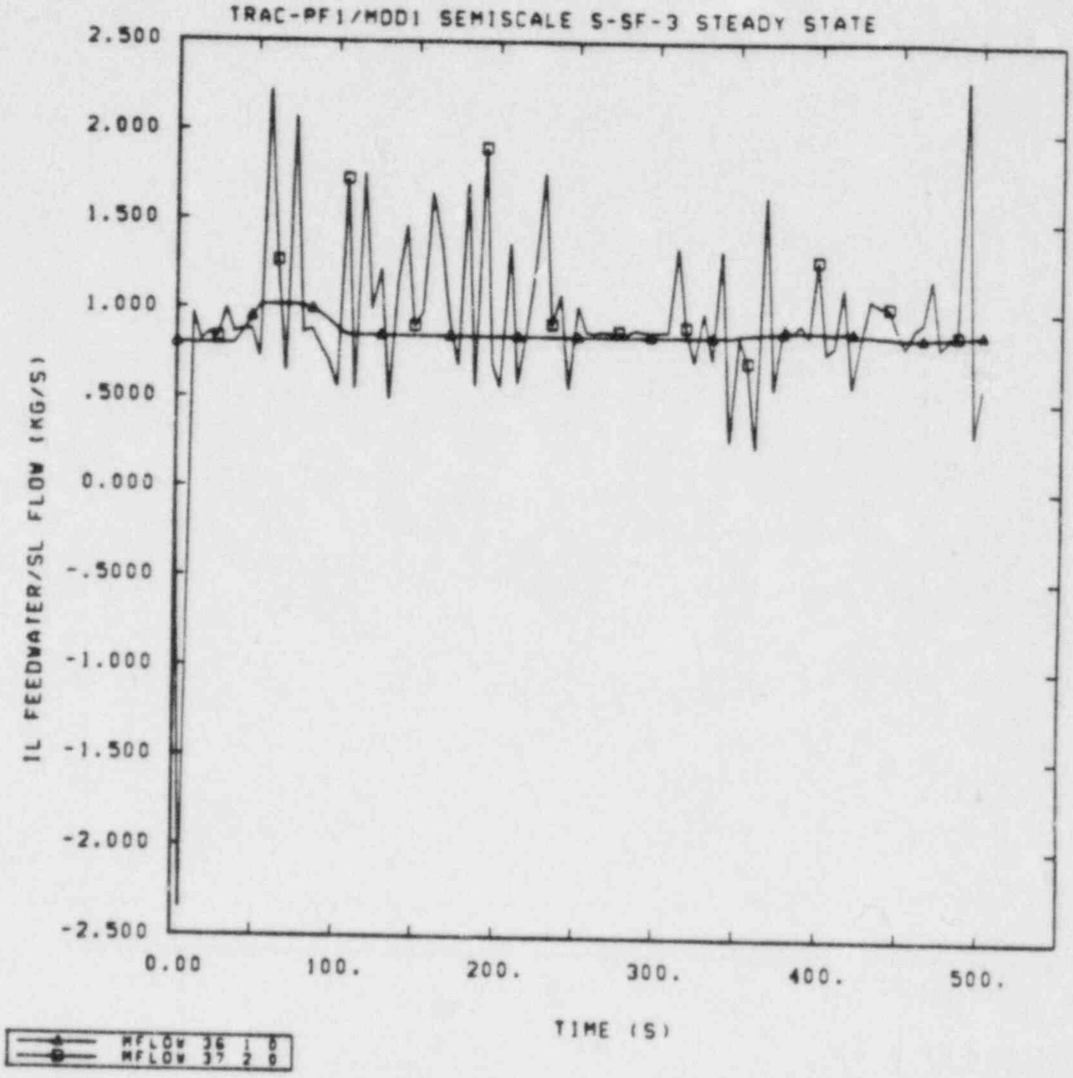

Figure 7.2.4 Intact Loop Feedwater and Steamline Flows

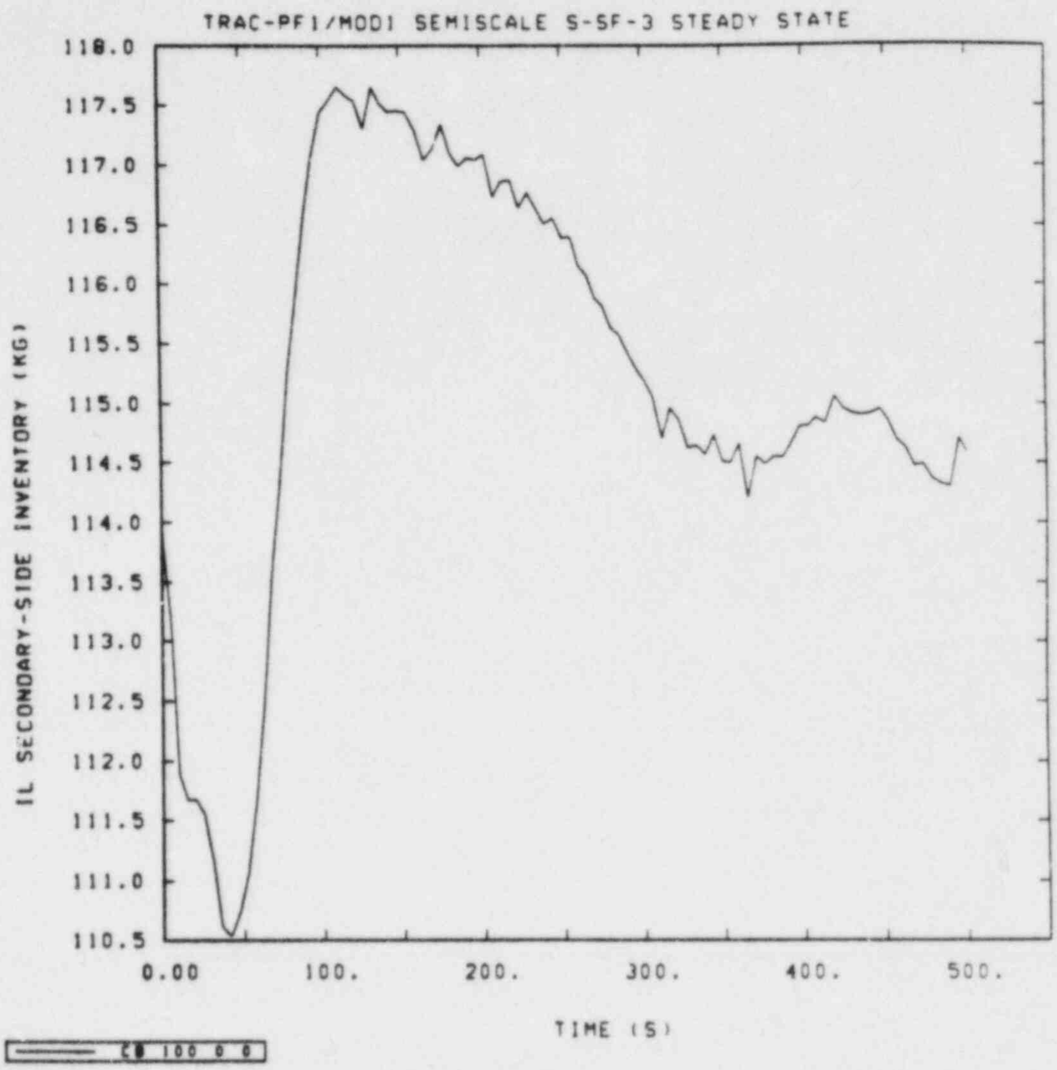

Figure 7.2.5 Intact Loop Secondary Side Inventory

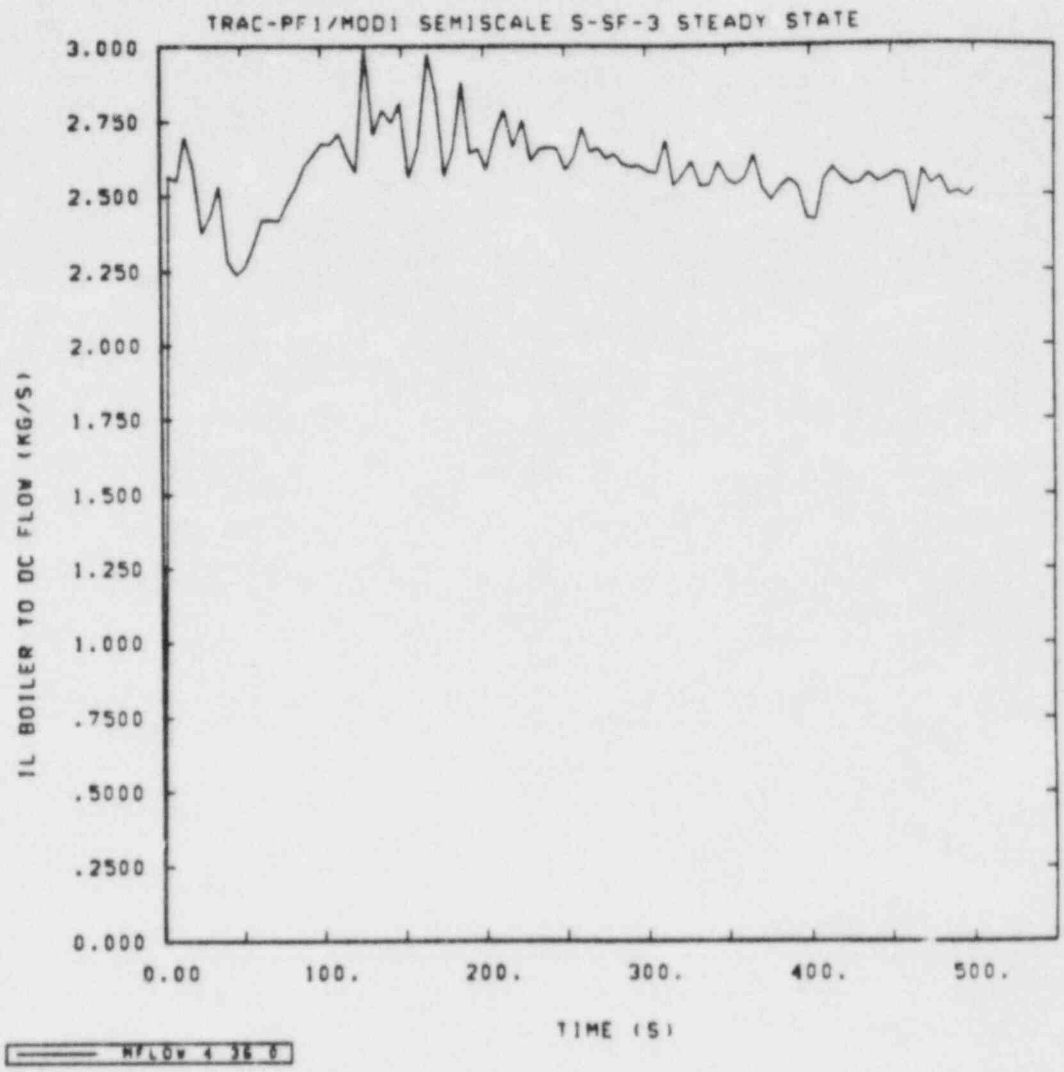

Figure 7.2.6 Boiler-to-Downcomer Flow in Intact Loop Steam Generator

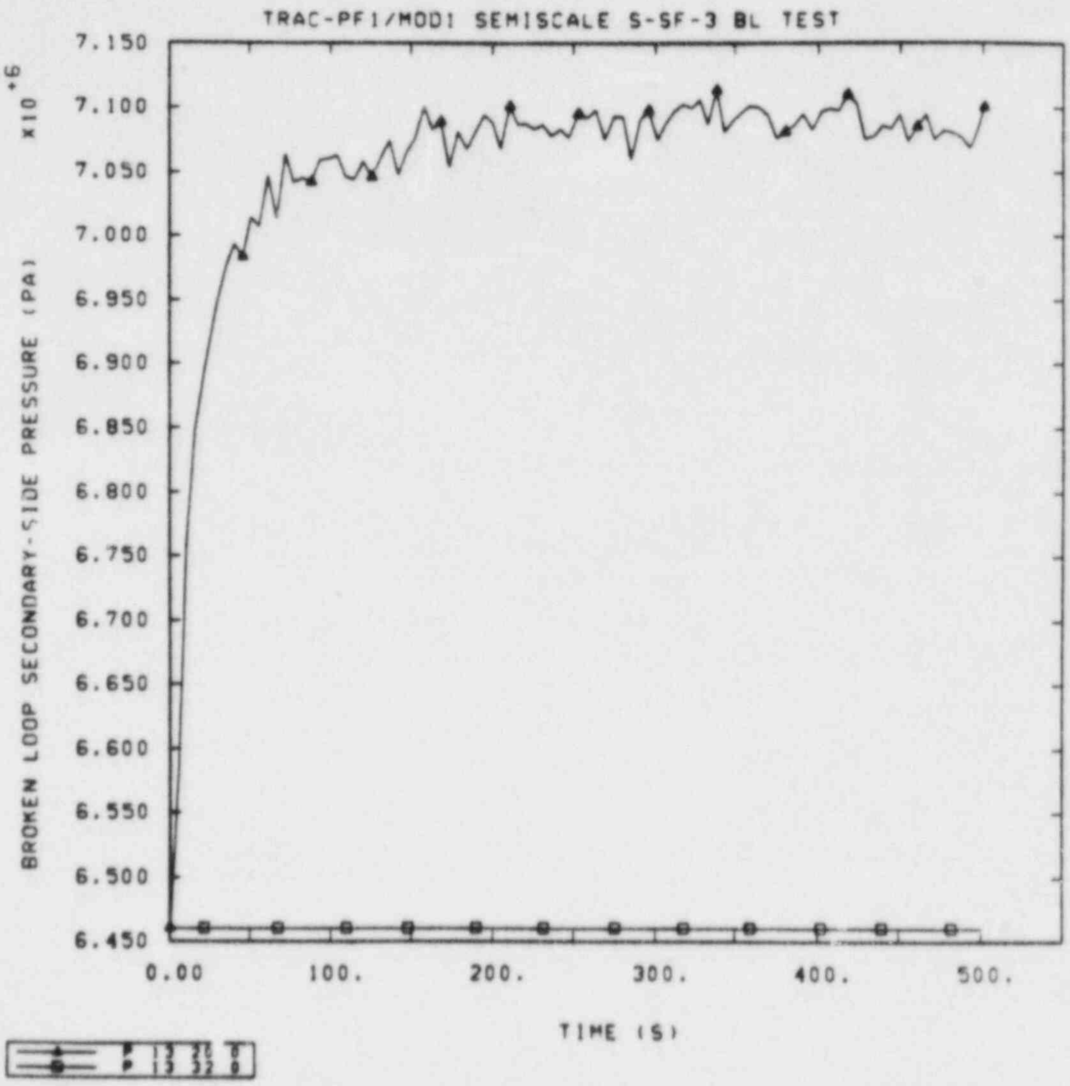

Figure 7 2.7 Broken Loop Secondary Side Pressure

8.0 REFERENCES

1. TRAC-PF1/MOD1: An Advanced Best-Estimate Computer Program for Pressurized Water Reactor Thermal-Hydraulic Analysis (Draft), Safety Code Development Group, Energy Division, Los Alamos National Laboratory, 1983.

2. S. L. Thompson et al., Thermal/Hydraulic Analysis Research Program Quarterly Report, October-December 1983, NUREG/CR-3329 (Vol. 4 of 4), SAND83-1171, Sandia National Laboratories, March 1984.

3. S. L. Thompson et al., Thermal/Hydraulic Analysis Research Program Quarterly Report, January-March 1984, NUREG/CR-3820 (Vol. 1 of 4), SAND84-1025, Sandia National Laboratories, June 1984.

4. D. Dobranich and L. D. Buxton, TRAC-PF1/MOD1 Independent Assessment: B&W 19-Tube Once-Through Steam Generator Tests, NUREG/CR-3877P, SAND84-1229, Sandia National Laboratories, July 1984.

5. R. K. Byers, TRAC-PF1/MOD1 Independent Assessment: Horizontal Stratified Flow Condensation Tests, NUREG/CR-????, SAND84-????, Sandia National Laboratories, to be published.

6. A. C. Peterson, TRAC-PF1/MOD1 Independent Assessment: NEPTUNUS Pressurizer Test Y05, NUREG/CR-3919, SAND84-1534, Sandia National Laboratories, to be published.

7. B. Brand, R. Kirmse and W. Winkler, OECD-CSNI Standard Problem No. 10: Refill and Reflood Experiments in a Simulated PWR Primary System (PKL), GRS report, December 1979.

8. D. Hein et al, PKL-Small Breaks (Test Series ID): Results of the Steady-State Test PKL ID1 in a Four-Loop Operation with 30 Bar System Pressure, KWU Tech. Rept. No. R 513/18/81, April 1981.

9. S. L. Thompson and L. N. Kmetyk, RELAP5 Assessment: PKL Natural Circulation Tests, NUREG/CR-3100, SAND82-2902, Sandia National Laboratories, January 1983.

10. I. S. Lim et al., Cocurrent Steam/Water Flow in a Horizontal Channel, NUREG/CR-2289, Northwestern University, August 1981.

11. H. A. Bloemen, Verification of the Pressurizer Model in RELAP5/MOD1, Energieonderzoek Centrum Nederland, Memo No. 0.375.10 GR 26 (OD 79-24), May 1983.

12. W. Riebold et al., Specifications: LOBI Pre-Prediction Exercise, Influence of PWR Primary Loops on Blowdown (LOBI), Technical Note No. I.06.01.79.25, Commission of the European Communities, J.R.C.-Ispra, February 1979.

13. L. Piplies and W. Kolar, Quick Look Report on LOBI Test A1-04R, Communication LQC 80-03, Commission of the European Communities, J.R.C.-Ispra, December 1980.

14. E. Ohlmer, Experimental Data Report on LOBI Test A1-04R, Communication LEC 80-03, Commission of the European Communities, J.R.C-Ispra, December 1980.

15. L. N. Kmetyk, RELAP5 Assessment: LOBI Large Break Transients, NUREG/CR-3075, SAND82-2525, Sandia National Laboratories, March 1983.

16. C. Addabbo, G. De Santi and L. Piplies, Quick Look Report on LOBI Test B-R1M, Communication LQC 82-08, Commission of the European Communities, J.R.C.-Ispra, March 1982.

17. T. Fortescue, LOBI Test B-R1M: Preliminary Data Report, Techn. Note No. I.06.01.81.153, Commission of the European Communities, J.R.C-Ispra, December 1981.

18. T. J. Boucher, Experiment Operating Specification for Semiscale Mod-2A Experiment S-IB-3, EGG-SEMI-5787, Idaho National Engineering Laboratory, February 1982.

19. T. J. Boucher and M. T. Leonard, Quick Look Report for Semiscale Intermediate Break Test S-IB-3, EGG-SEMI-6013, Idaho National Engineering Laboratory, August 1982.

20. K. E. Sackett and L. B. Clegg, Experiment Data Report for Semiscale Mod-2A Intermediate Break Test Series (S-IB-3), NUREG/CR-2738, EGG-2198, Idaho National Engineering Laboratory, June 1982.

21. D. J. Shimeck, Experiment Operating Specification for Semiscale Mod-2A Steam and Feedwater Line Break Scoping Experiment Series, EGG-SEMI-5830, Idaho National Engineering Laboratory, March 1982.

22. D. J. Shimeck, L. J. Martinez and G. R. Berglund, Quick Look Report for Semiscale Feedwater Line Break Tests S-SF-1, S-SF-2 and S-SF-3, EGG-SEMI-5940, Idaho National Engineering Laboratory, July 1982.

23. Thomas M. O'Connell, Experiment Data Report for Semiscale Mod-2A Feedwater Line Break Experiments (Tests S-SF-1, S-SF-2, and S-SF-3), NUREG/CR-2912, EGG-2216, Idaho National Engineering Laboratory, September 1982.

DISTRIBUTION:

Division of Technical Information
  and Document Control
NRC Distribution Contractor
U. S. Nuclear Regulatory Commission
15700 Crabbs Branch Way
Rockville, MD 20850
        300 copies for R4

U. S. Nuclear Regulatory Commission (4)
Reactor Systems Research Branch
Division of Accident Evaluation
Office of Nuclear Regulatory Research
7915 Eastern Avenue
Silver Spring, MD 20910
Attn: Louis M. Shotkin
      Fuat Odar
      R. Landry
      H. S. Tovmassian

EG&G Idaho (6)
Idaho National Engineering Laboratory
P. O. Box 1625
Idaho Falls, ID 83415
Attn: T. R. Charlton
      G. W. Johnsen
      Edna Johnson
      L. Feinauer
      V. H. Ransom
      R. J. Wagner

Thad D. Knight
Dennis R. Liles
Los Alamos National Laboratory (2)
K553 Q-9
Los Alamos, NM 87545

P. Saha, 130
Department of Nuclear Energy
Brookhaven National Laboratory
Associated Universities, Inc.
Upton, New York 11973

N. H. Shah
Babcock & Wilcox Co. (NPGD)
P. O. Box 1260
Lynchburg, VA 24505

Jesse Fell (5)
Deputy Director, Water Reactor Programs
Atomic Energy Establishment
Winfrith
Dorchester, Dorset DT28DH
ENGLAND

6400 A. W. Snyder
6410 J. W. Hickman
6417 D. C. Carlson
6420 J. V. Walker
6421 T. R. Schmidt
6422 D. A. Powers
6423 P. S. Pickard
6425 W. J. Camp
6427 M. Berman
6440 D. A. Dahlgren
6442 W. A. von Riesemann
6444 S. L. Thompson (17)
6444 L. D. Buxton
6444 R. K. Byers
6444 R. K. Cole, Jr.
6444 P. N. Demmie
6444 D. Dobranich
6444 M. G. Elrick
6444 L. N. Kmetyk
6444 R. Knight
6444 J. M. McGlaun
6444 J. Orman
6444 A. C. Peterson
6444 W. H. Schmidt
6444 R. M. Summers
6444 S. W. Webb
6449 K. D. Bergeron
3141 C. M. Ostrander (5)
3151 W. L. Garner
8024 M. A. Pound

NRC FORM 335 (2-84) NRCM 1102, 3201, 3202

U.S. NUCLEAR REGULATORY COMMISSION

BIBLIOGRAPHIC DATA SHEET

SEE INSTRUCTIONS ON THE REVERSE

1. REPORT NUMBER (Assigned by TIDC, add Vol. No., if any) NUREG/CR-3820 SAND84-1025/2 of 4	3. LEAVE BLANK
2. TITLE AND SUBTITLE Thermal/Hydraulic Analysis Research Program Quarterly Report April-June 1984	4. DATE REPORT COMPLETED MONTH: July YEAR: 1984
5. AUTHOR(S) S. L. Thompson, Person in Charge	6. DATE REPORT ISSUED MONTH: August YEAR: 1984
7. PERFORMING ORGANIZATION NAME AND MAILING ADDRESS (Include Zip Code) Thermal/Hydraulic Analysis Division 6444 Sandia National Laboratories P. O. Box 5800 Albuquerque, NM 87185	8. PROJECT TASK WORK UNIT NUMBER 9. FIN OR GRANT NUMBER A-1205 and A-1374
10. SPONSORING ORGANIZATION NAME AND MAILING ADDRESS (Include Zip Code) Reactor Systems Research Branch Division of Accident Evaluation Office of Nuclear Regulatory Research U. S. Nuclear Regulatory Commission Washington, DC 20555	11a. TYPE OF REPORT Technical, Quarterly b. PERIOD COVERED (Inclusive dates) April - June 1984
12. SUPPLEMENTARY NOTES	
13. ABSTRACT (200 words or less)	
14. DOCUMENT ANALYSIS - a. KEYWORDS/DESCRIPTORS b. IDENTIFIERS/OPEN ENDED TERMS	15. AVAILABILITY STATEMENT Unlimited 16. SECURITY CLASSIFICATION (This page) Uncl (This report) Uncl 17. NUMBER OF PAGES 54 18. PRICE

120555078877 1 1AN1R4
US NRC
ADM-DIV OF TIDC
POLICY & PUB MGT BR-PDR NUREG
W-501
WASHINGTON DC 20555